Fall 12-5-2014

A Niobium Deposit Hosted by a Magnetite-Dolomite Carbonatite, Elk Creek Carbonatite Complex, Nebraska, USA

Michael J. Blessington
University of Nebraska-Lincoln, michael.blessington@huskers.unl.edu

A NIOBIUM DEPOSIT HOSTED BY A MAGNETITE-DOLOMITE CARBONATITE, ELK CREEK CARBONATITE COMPLEX, NEBRASKA, USA

by

Michael J. Blessington

A THESIS

Presented to the Faculty of

The Graduate College at the University of Nebraska

In Partial Fulfillment of Requirements

For the Degree of Master of Science

Major: Earth and Atmospheric Sciences

Under the Supervision of Professor Richard M. Kettler

Lincoln, Nebraska

December, 2014

A NIOBIUM DEPOSIT HOSTED BY A MAGNETITE-DOLOMITE CARBONATITE, ELK CREEK CARBONATITE COMPLEX, NEBRASKA, USA

Michael Joseph Blessington, M.S.

University of Nebraska, 2014

Adviser: Richard M. Kettler

The Elk Creek Carbonatite Complex (ECCC) is a large Early Cambrian carbonatite complex that intrudes Precambrian basement rocks in Southeast Nebraska. This dolomitic carbonatite complex includes a magnetite-dolomite rock with accessory barite, ilmenite, rutile, and quartz. This rock is identified by a characteristic enrichment in niobium due to accessory pyrochlore mineralization in the form of disseminations and inclusions in ilmenite and magnetite. Pyrochlore is also present in other carbonatite rocks in the complex as an accessory mineral with sporadic local high-grade intercepts in drill cores.

Carbonatite rock samples are characterized by transmitted-light microscopy, cathodoluminescent microscopy, backscattered electron imaging (BEI), and whole-rock geochemical analysis by XRF and ICP-AES. The typical texture for the magnetite-dolomite carbonatite is a matrix of fine-grained magnetite, ilmenite, barite, and dolomite with clasts of dolomite carbonatite; these clasts can appear as elongate lenticular bodies or angular fragments. Cross-cutting relationships with other carbonatite rocks in the complex show that the emplacement of this rock was an early event in the ECCC. Whole-rock chemical analysis indicates unusual HFSE geochemistry relative to other

carbonatite rocks in the ECCC.The geology and chemistry of this rock is also unusual in comparison to carbonatite rocks worldwide. A discreet pulse of reduced, iron-rich carbonatite magma is proposed as the origin for the magnetite-dolomite carbonatite.

Pyrochlore grains in magnetite-dolomite carbonatite and in other carbonatite rocks in the complex are characterized by transmitted-light microscopy, BEI, and microprobe chemistry analysis. Observations drawn from transmitted light microscopy and BEI indicate three different types of pyrochlore present in the Elk Creek Carbonatite Complex: (1) 0.2-2 mm diameter euhedra with oscillatory zoning, (2) unzoned 10-100 μm diameter euhedra, and (3) <10 μm diameter anhedra which occur as inclusions in ilmenite and magnetite. The chemistry of each of the three types of pyrochlore is distinct. Type 1 is enriched in Ta, Type 2 is near-stoichiometric pyrochlore, and Type 3 is enriched in Sr and Ti. The characteristic niobium enrichment in the magnetite-dolomite carbonatite is largely due to the presence of Type 3 pyrochlore. Type 3 pyrochlore formed early in the formation of the magnetite-dolomite carbonatite.

DEDICATION: I would like to dedicate this work to the memory of my father, William K. Blessington, who helped spark my interest in geology as a child and who encouraged me to pursue that interest professionally.

ACKNOWLEDGEMENTS: I would like to first thank my major adviser, Dr. Richard M. Kettler, and my thesis committee members, Dr. Caroline Burberry, and Dr. Ronald Goble, for substantial help and support over the past two years in making this product.

I would like to acknowledge Dr. Phil Verplanck of the USGS for the whole-rock geochemistry data sets used in this work, as well as additional assistance. I would also like to thank Dr. G. Lang Farmer of the USGS for help with this work. This work, however, is not the final report required by the USGS Mineral Resources External Research Program (MRERP) and Drs. Farmer and Verplanck are not responsible for any errors or omissions in this work.

I would like to thank Dr. Julian Allaz (UC Boulder) and Heather Lowers (USGS Denver) for facilitating microprobe chemistry measurements and backscattered electron imaging. I would also like to thank Dr. Tracy Frank (UNL Earth and Atmospheric Sciences Dept.) for allowing me to use her microscopy lab to collect transmitted-light and CL images.

Thank you to Dr. Melanie Werdon and the Alaska Division of Geological and Geophysical Surveys for sparking my interest in REE and niobium geology.

Finally, I would like to acknowledge the support of my family, especially my mother, Lynn Wibbenmeyer, and my stepfather, Merlin Wibbenmeyer. I would also like to thank Erin Lange and Kelsey Post for substantial support and encouragement over the past two years.

GRANT INFORMATION: Major funding for my work was provided by the USGS's Mineral Resources External Research Program and a teaching assistantship from the UNL Dept. of Earth and Atmospheric Sciences.

Additional funding was provided by a GSA Graduate Student Research Grant, and the Nebraska Geological Society's Yatkola-Edwards Award.

Table of Contents

List of Figures

List of Tables

1. Introduction

Carbonatites and carbonatite-associated rocks comprise the predominant source of niobium oxides in the world, with a handful of carbonatites in Brazil and Canada responsible for nearly all of the world's production (Mitchell, 2014). Additional reserves in South America, the Kola Peninsula, and Africa are also principally carbonatite-related, with a minor additional contribution from syenitic/peralkaline systems and pegmatites (Mitchell, 2014). Pyrochlore is the predominant ore mineral for carbonatite niobium deposits (Mitchell, 2014). Experimental petrography as well as field studies suggest that pyrochlore is a magmatic mineral which forms early in the ascent and emplacement of a carbonatite melt, with the rheology of the carbonatite melt being the primary control on spatial distribution (Mitchell and Kjarsgaard, 2004; Mitchell, 2014). It is a common accessory mineral in carbonatites and has a molecular structure with an enormous capacity for substitution which will reflect geochemical trends in an igneous fluid as well as indicate secondary alteration or weathering (Atencio, 2010).

The Elk Creek Carbonatite Complex (ECCC) is a large intrusive carbonatite system located in Southeast Nebraska, 75 km southeast of Lincoln and 110 km south of Omaha (Fig. 1). Exploratory drilling by Molycorp in the 1970s and 1980s intercepted a niobium resource in the center of the ECCC hosted by an unusual magnetite-dolomite carbonatite rock (Mariano, 1978). Magnetite and dolomite are the major rock-forming minerals in this rock lithology, with minor ilmenite, rutile, biotite, quartz, and pervasive barite alteration. The magnetite-dolomite carbonatite exhibits several different textures but is typically fine-medium-grained and very dark in hand sample. Frequently, the

magnetite-dolomite carbonatite is a rock with clasts of dolomite carbonatite contained within, either as angular fragments or as elongate lenticular clasts.

In this paper we describe the carbonatite and silicate lithologic units of the ECCC, with a focus on the magnetite-dolomite carbonatite. Based on compiled Molycorp logs, observed cross-cutting relationships, and geochemistry, we propose an order of emplacement for the carbonatite and silicate rocks in the complex. New measurements of the whole-rock geochemistry of ECCC lithologies indicates that the magnetite-dolomite carbonatite is chemically unique relative to the other rocks in the complex, and propose that this rock is the product of a pulse of iron-rich carbonated magma which intruded into the ECCC during its formation. We also describe the various alteration styles observed in the ECCC, which indicate a trend of increasingly oxidizing and sulfur-rich fluids that overprinted the carbonatite and silicate rocks.

Superficially, the magnetite-dolomite rock bears some similarity to both phoscorites and nelsonites, rare iron-rich igneous rocks with magnetite as a major rock-forming mineral (Krasnova et al., 2004). We compare the magnetite-dolomite carbonatite rock to these rock types on the basis of chemistry and mineralogy, identifying critical differences which may single out the magnetite-dolomite carbonatite as a unique rock. We also consider the potential petrogenesis of the magnetite-dolomite carbonatite in light of the genetic models proposed for comparable rock types.

The niobium resource in the Elk Creek Carbonatite is contained in pyrochlore, an accessory mineral throughout the complex (Mariano, 1978). Multiple “generations” of pyrochlore mineralization in the ECCC were originally described by Molycorp geologists

in the 1970s and 1980s (Mariano, 1978). In boreholes EC-11 and EC-15, Mariano (1978) identified four types of pyrochlore based on optical characteristics and spectral analysis. We reconsider this classification scheme in light of new chemistry obtained by electron microprobe, and reclassify pyrochlore at Elk Creek into three types based on morphology, spatial occurrence, and chemistry: A large, euhedral, Ta-rich Type 1; a stoichiometric and euhedral Type 2, and an anhedral <10 μm diameter Type 3 limited to the magnetite-dolomite carbonatite and typically included in ilmenite and magnetite. We also propose a paragenetic order for pyrochlore in the magnetite-dolomite carbonatite, with special attention to pyrochlore hosted in ilmenite and magnetite.

2. Geologic Setting and Exploration History

The Elk Creek Carbonatite Complex is located on the eastern margin of the 1.1 Ga Midcontinent Rift System (MRS), one of two major tectonic structures in the basement rocks of southeastern Nebraska (Fig. 1). This rift system was active for slightly more than 20 million years before volcanism and extensional faulting ended (Ojakangas et al., 2001). This period was marked by the emplacement of voluminous flood basalts and associated gabbroic intrusive bodies (Ojakangas, 2001). The western arm of the MRS extends for 1300 km from the Lake Superior Basin to Northern Kansas along a northeast-southwest axis (Ojakangas et al., 2001). The rift cuts through the basement rocks of southeastern Nebraska along that axis, with an transfer zone displacing the rift near the Nebraska-Kansas border (Carlson and Treves, 2005). The flood basalts and subsequent infill have been mapped by geophysics and borehole intercepts but are not exposed at the surface in Nebraska (Carlson and Treves, 2005). Southeastern Nebraska also comprises

the northern extent of the Nemaha Ridge uplift structure, an Ancestral Rockies-age tectonic feature running roughly N-S through Nebraska, Kansas, and Oklahoma (Carlson and Treves, 2005). The Elk Creek Carbonatite is located in the northernmost portion of the Nemaha uplift and was likely exposed at the surface during the uplift event (Carlson and Treves, 2005).

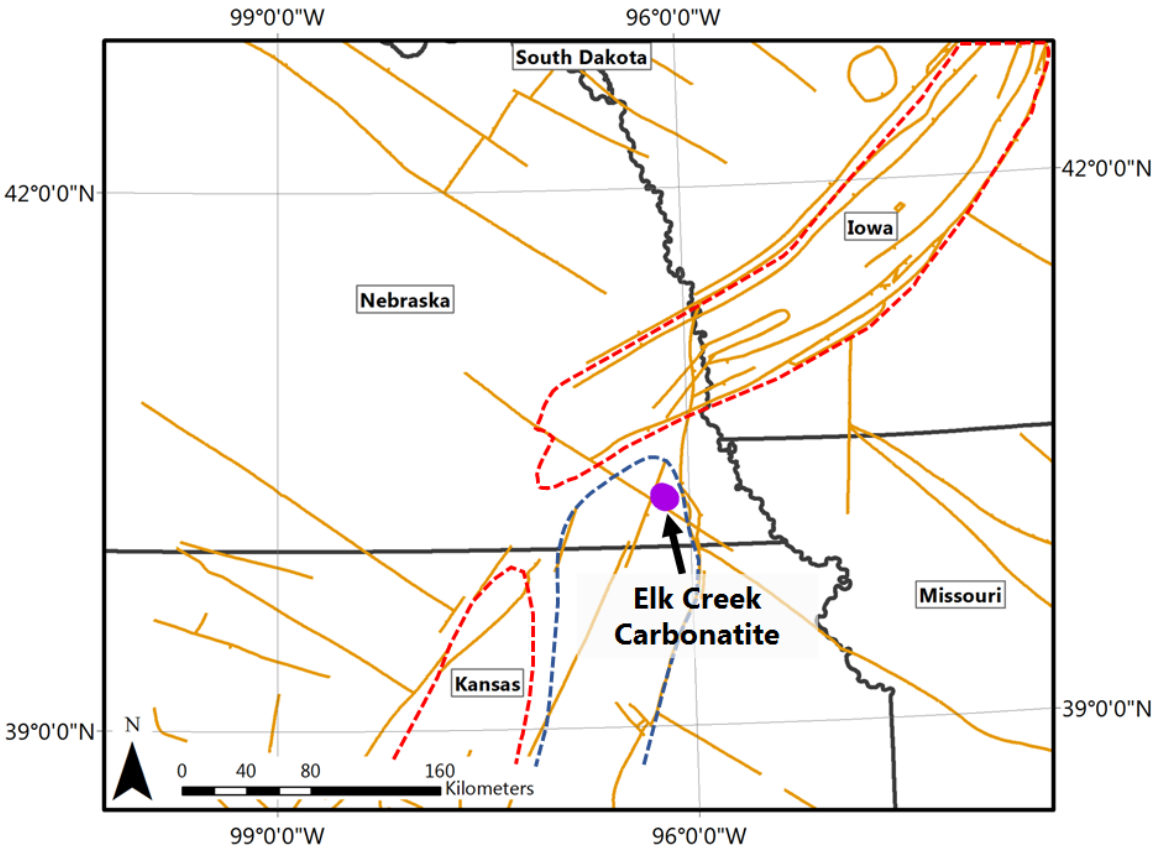

Fig. 1: Location of the Elk Creek Carbonatite Complex in relation to the Midcontinent Rift System. Midcontinent Rift System polygon (red dashed outline) adapted from Ojakangas et al. (2001). Nemaha Uplift/Nemaha Ridge polygon (blue dashed outline) adapted from Steeples et al. (1979). Fault lines (orange) adapted from Dicken et al. (2001)

The basement/country rocks that surround the ECCC consist of metamorphic and igneous rocks of Precambrian age, including granites, diorites, gabbros, schists, and gneisses (Xu, 1996). In the vicinity of the complex, the depth to crystalline basement rock is typically 150-250m. The gneisses and schists are approximately 1.8 billion years old and were accreted to Laurentia during the Central Plains Orogeny (Sims and Petermar, 1986). The metamorphic rocks associated with this tectonic event are largely amphibolite-facies and have a NW-SE structural trend defined by linear magnetic and gravity anomalies (Sims and Petermar, 1986). The granites are a product of multiple emplacement styles at 1.7 and 1.4 Ga. The older granites arethe product of island arc accretion, whereas the younger granites are anorogenic Rapikivi-type intrusions (Sims and Petermar, 1986). The gabbros were emplaced at approximately 1.2 Ga and are associated with Midcontinent Rift magmatism (Carlson and Treves, 2005).

2.1 The Elk Creek Carbonatite

The Elk Creek Carbonatite Complex is not exposed at the surface, and is covered by 10-15 m of quaternary glacial till/loess and 180 m of cyclic Pennsylvanian carbonate and clastic sedimentary rocks. The depth to the carbonatite varies depending on the surface topography and the uneven paleosurface. The ECCC is stock-like and roughly elliptical in plan view (Fig. 2) with a diameter of 6-8 km and a truncated roof with a thin weathering zone (Drenth, 2014). The deepest drill holes (approximately 800 meters measured depth at -90 degrees inclination) have ended in carbonatite. Drenth (2014) interpreted gravity and aeromagnetic data as evidence that the intrusion is funnel-shaped, opening towards the surface. The principle niobium mineralization zone at Elk Creek is

located near the center of the intrusion and is small relative to the carbonatite complex, comprising less than 2% of the volume of the entire intrusive complex (Drenth, 2014).

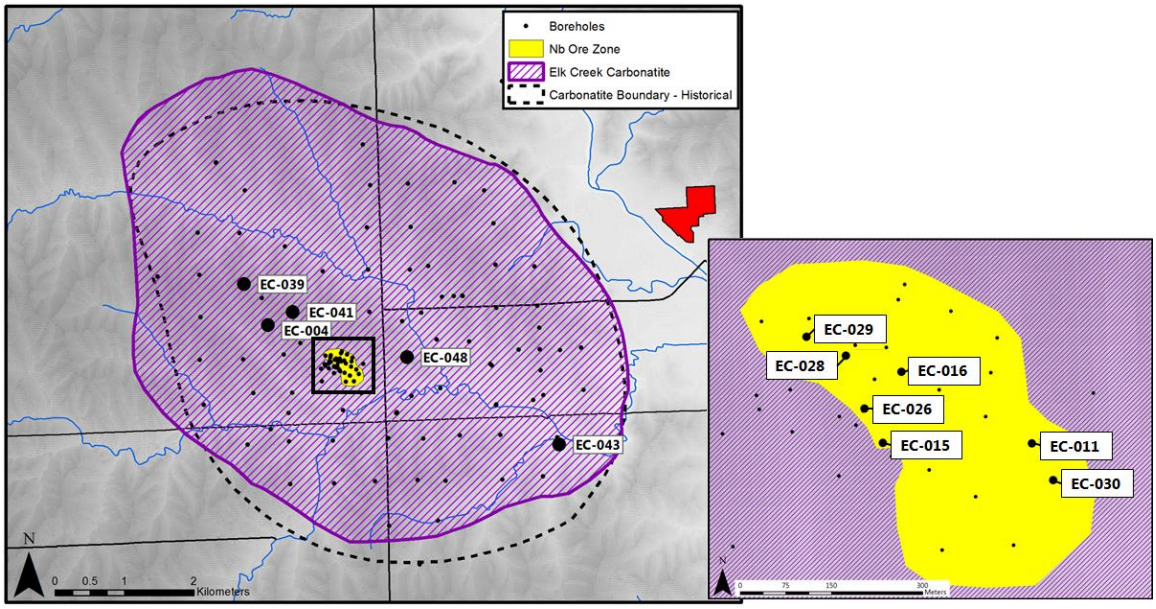

Fig. 2: Spatial extent of the Elk Creek Carbonatite. Purple boundary is based on 2011 geophysical surveys and adapted from Drenth (2014). The historical boundary is based on Molycorp estimations (P.C.J., 1985). Boreholes sampled for this project are labeled.

The zone of mineralization is associated with a strong aeromagnetic and gravity high that contrasts well with the surrounding carbonatite rocks (Drenth, 2014). Drenth (2014) concluded that the magnetic anomaly associated with niobium mineralization continues at depth; the volume of magnetite-dolomite carbonatite as estimated solely from borehole intercepts is insufficient to explain the gravimetric and magnetic anomaly at the center of the complex. Additional drilling would be expected to intercept more magnetite-bearing carbonatite at deeper levels (Drenth, 2014).

K/Ar dating of biotite from the silicate rocks in the ECCC by the USGS in the mid-1980s yielded an age of 544 ± 7 Ma (Peterman, personal communication, 1985; reported by Carlson and Treves, 2005). Subsequent work from Georgia State University on biotite from the mafic dike rock produced ages of 464 ± 5 and 484 ± 5 Ma (Ghazi, personal communication; reported by Carlson & Treves, 2005). New U-Pb analysis of zircons from the syenite yielded ages of 480 ± 20 Ma and 540 ± 14 Ma (Farmer et al., 2013). Whole-rock Sm-Nd isochrons from the ECCC carbonatite rocks confirm this approximate range of dates (Farmer et al., 2013).

The Elk Creek Carbonatite was discovered after regional geophysical surveying by the State of Nebraska located a large circular magnetic and gravity anomaly that was subsequently drilled by the State and the US Bureau of Mines (Carlson and Treves, 2005). Cominco America initiated the first phase of industry exploration of the ECCC (Carlson and Treves, 2005). Molycorp Inc. obtained exploration rights to the property in the mid-1970s and drilled over 24,000 meters of core from 106 drill holes between 1977 and 1986 (boreholes EC-1 to EC-106). The split core and corresponding 10’ composite chip samples drilled by Molycorp were later donated to the University of Nebraska-Lincoln and released into the public domain. This donation also includes geological core logs, drilling reports, and internal geological reports prepared by Molycorp. The mineral rights for the ECCC are currently held by Niocorp Inc., and exploratory drilling, resource estimation, and geotechnical analysis is ongoing.

3. Methods

Petrological and mineralogical characterization of the lithologies in the ECCC was performed on thin sections by transmitted-light microscopy utilizing a polarizing microscope, cathodoluminescent microscopy, and backscattered/secondary-electron imaging. Characterization of niobium pyrochlore mineralization was also performed using these techniques. Thin-section samples were selected based on whole-rock niobium grade as measured by Molycorp and reported in borehole logs, representativeness with respect to the surrounding lithology, and the relative absence of visible alteration. All thin-sections were ground to a thickness of 30 μm and polished for microprobe analysis.

Mineral chemistry analyses were performed in two phases for this evaluation. For Type 1 pyrochlore, magnetite, ilmenite, and rutile, a JEOL 8900 electron microprobe was used at the USGS Denver Microbeam Laboratory. The spot size was 10 μm for Type 1 pyrochlore grains and 5 μm for magnetite, ilmenite, and rutile; a 20 kV beam at 50 nA was used for all analyses. Type 2 and 3 pyrochlore grains were analyzed using a JEOL JXA 8600 electron microprobe at the University of Colorado - Boulder. Spot size for these analyses was 5 μm and beam power was 20 kV at 50 nA. For pyrochlore grains with a diameter <10 μm, a focused beam (<5 μm) was used. Additional mineral geochemistry data were obtained by energy dispersive spectral analysis during these experiments.

Thirty-four samples of carbonatite and carbonatite-associated silicate rocks, including 5 samples of magnetite-dolomite carbonatite from drill cores EC-11, EC-16, EC-28, and EC-29 were obtained from crushed rock composite samples derived from 3.05 m (10’) intervals of mechanically-split core. These samples were split, pulped, and

analyzed at the USGS laboratory in Denver, CO. Major elements were analyzed using X-ray fluorescence (XRF) whereas minor and trace elements were measured using ICP-MS and ICP-AES techniques. Selected whole-rock analysis from lithologically representative samples are presented in appendix A.

4. Geology of the ECCC

4.1 Lithologic Units

The Elk Creek Carbonatite is lithologically diverse and contains a suite of different dolomite carbonatite rocks with distinct mineral assemblages and textures. The complex also contains significant late-stage intrusion by narrow mafic dikes and veins, and moderate-to-pervasive secondary alteration across large core intercepts. Common alteration minerals are barite, apatite, dolomite, hematite and limonite; less common are calcite and chlorite. Some of these alteration zones surround displacement planes/fault zones as well as mafic dikes. Historical names assigned by Molycorp are presented for reference. Observations are primarily drawn from re-examination and re-logging of split core intervals originally logged by Molycorp workers, and polished thin sections produced from lithologically representative core samples.

4.1.1 Dolomite Carbonatite: The most volumetrically abundant unit in the Elk Creek carbonatite is a massive dolomite carbonatite (Molycorp: Apatite Beforsite). This unit has variable texture, ranging from a fine-grained flow-banded rock to a coarse-grained carbonatite rock with large prismatic dolomite crystals (Fig. 3). The color varies, and ranges from white to beige to grey in unaltered intervals. Dolomite is the major rock-

forming mineral with minor apatite ± fluorite and accessory pyrite, pyrochlore, hematite, ilmenite, and magnetite. Barite is observed in relatively-unaltered dolomite carbonatite as sparse veinlets and patches (Fig. 3).

Fig. 3: Hand-sample image of coarse-grained dolomite carbonatite with pale red-pink veinlets and patches containing fine-grained dolomite, barite and apatite. Sparse fine-grained sulfides are disseminated throughout, typically pyrite (EC-43 1069').

In thin-section, the rock is most typically holocrystalline with equant anhedral dolomite grains, and is almost pure dolomite in unaltered intercepts. Thin veinlets are widespread in this rock; vugs and open spaces are less widespread and are typically localized. Distribution of pyrochlore is variable in the dolomite carbonatite; typically, pyrochlore is 0.1% or less by modal volume, but meter-scale intercepts can contain localized areas of resource-grade niobium mineralization. Niobium grades of 1.6% Nb_2O_5 were measured in a three-meter-long composite sample of dolomite carbonatite from drill hole EC-39 (EC-39 2030', Table A1). The niobium grades for the rocks both

immediately above and below this three-meter section are at background (<0.1% Nb_2O_5) (Sherer, 1984a).

A dolomite carbonatite variant (Molycorp: Apatite Beforsite II) is seen in some cores at Elk Creek (Sherer, 1984a). This carbonatite unit is similar to the more widespread dolomite carbonatite, but contains biotite and phlogopite (frequently altered to chlorite), silicates, pyrite, and chalcopyrite (Fig. 4). Sherer (1984a) identifies the silicate minerals as orthoclase and aegerine. The color of this rock is typically redder than unaltered dolomite carbonatite or earlier apatite-altered dolomite carbonatite. Texture is fine-to-medium-grained and occasionally lineated. This unit has no consistently-significant niobium mineralization based on Molycorp assays, nor have significant concentrations been observed in thin section or hand sample. The one exception is a mineralized intercept 10 meters long reported in borehole EC-39 at a depth of 470m (1550'). This intercept was described as containing disseminated <1.5 mm yellow pyrochlore with a measured whole-rock Nb_2O_5 grade ranging from 0.54% to 0.70% (Sherer, 1984a).

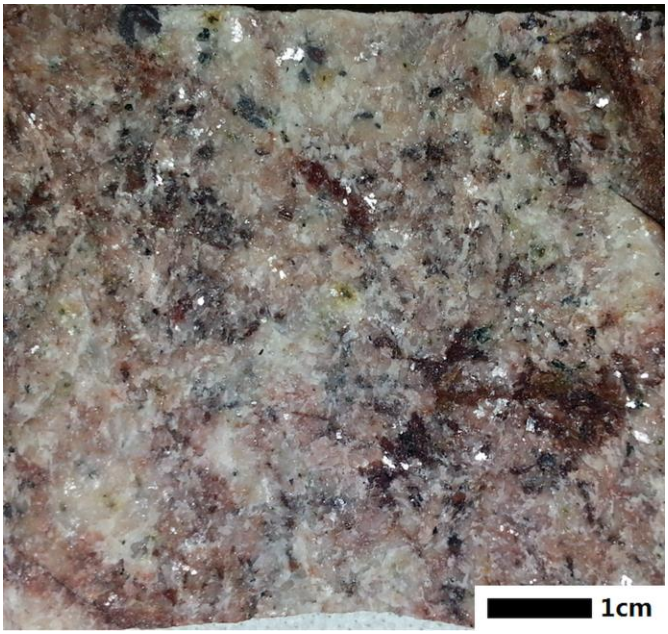

Fig. 4: Hand-sample image of medium-grained dolomite carbonatite with disseminated fine-medium-grained biotite and chlorite after biotite (black elongated crystals). Minor pervasive barite alteration with patches of medium-grained barite crystals at lower middle-right (EC-41 1761')

4.1.2 Apatite-Dolomite Carbonatite: Dolomite carbonatite with significant apatite mineralization is typically a localized feature in the Elk Creek Carbonatite based on core intercepts. This mineralization is not uniform across these intercepts; nearly pristine dolomite carbonatite will grade rapidly into centimeter-scale zones consisting of more than 10% apatite grains by modal volume. These apatite-rich zones consist of altered fine-to-medium-grained dolomite with elongate rounded-subrounded apatite as a secondary mineral (Fig. 5). In transmitted light, altered dolomite adjacent to apatite has a cloudy, grainy appearance and is nearly opaque in some areas (Fig. 5). This cloudy

appearance is not observed in apatite, and dolomite grains in contact with apatite have concave grain boundaries that are not seen in unaltered dolomite carbonatite.

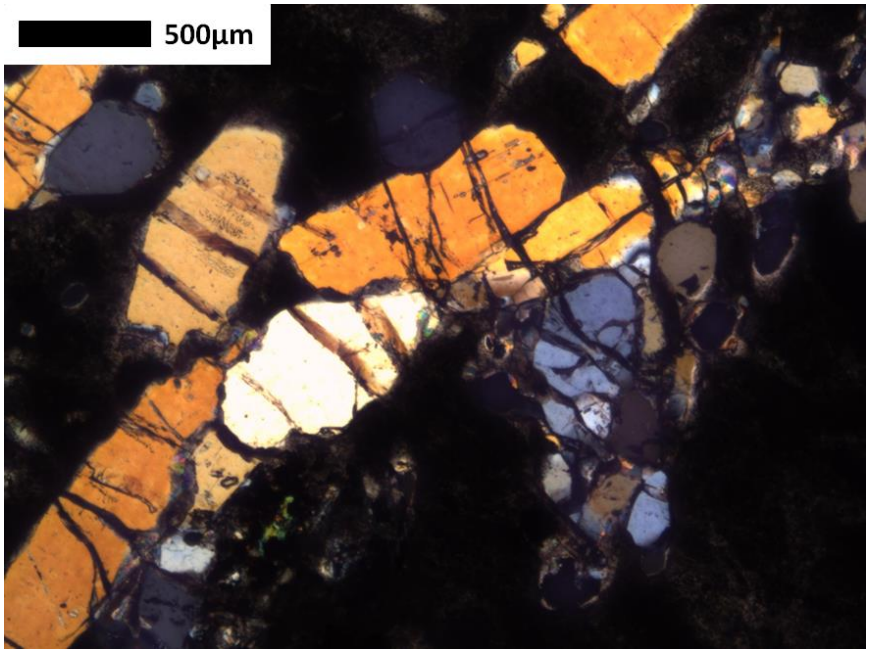

Fig. 5: Cross-polarized light image of large ovoid apatite grains in altered dolomite carbonatite. Altered dolomite has a dark appearance in cross-polarized light; optical characteristics such as birefringence are partially obscured (EC-10 1493')

4.1.3 Magnetite-Dolomite Carbonatite: The principal niobium ore rock is a magnetite-bearing dolomite carbonatite (Molycorp: Magnetite Beforsite) (Fig. 6A-C). This rock is fine-grained, dark, and in most instances is marked by a porphyry-like texture with elongate-lenticular 1-2 cm light-grey clasts of fine-medium grained dolomite in a matrix of nearly-black fine-grained magnetic rock (Fig. 6A). These elongate clasts have a preferential orientation and will appear roughly parallel in core, giving the appearance of flow banding or shearing (Fig. 6A). Equant sub-rounded clasts are less abundant but occur in some intervals in localized zones adjacent to elongate clasts. This

unit also occurs as a massive rock cut by thin veinlets (Fig. 6B), and as a breccia with a magnetite-dolomite carbonatite matrix (Fig. 6C).

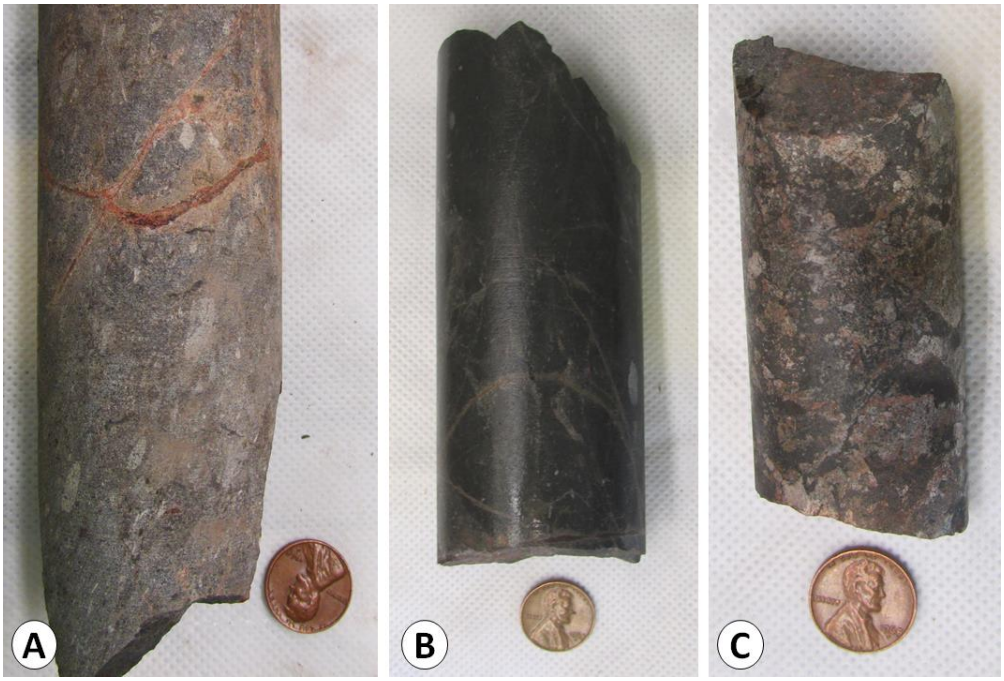

Fig. 6: Hand-sample images of magnetite-dolomite carbonatite textures. (A) Rounded-subrounded elongate clasts oriented along a dominant lineation plane with a magnetite-dolomite carbonatite matrix. Contrast adjusted to show texture (EC-28 1984'). (B) Veinleted with a few rounded/porphyritic clasts. Core is strongly magnetic in this sample (EC-28 2059'). (C) Brecciated texture with magnetic matrix material (EC-11 2429').

The light-colored clasts in the porphyritic magnetite-dolomite carbonatite are fine-grained holocrystalline blebs composed of equigranular anhedral dolomite (Fig. 7A) with minor biotite (Fig. 7B), ovoid apatite, and euhedral pyrochlore. The very dark matrix is difficult to study under transmitted light due to the high concentration of opaque minerals (Fig. 7A, 8A) but the primary rock-forming minerals are identified from

backscattered electron imaging and energy dispersive spectrometry as magnetite, ilmenite, dolomite, and barite with minor apatite, rutile, biotite, quartz, and pyrochlore. Dolomite in the matrix occurs interstitial to magnetite and ilmenite (Fig.7B). In cathodoluminescent microscopy, the dolomite becomes darker toward the edges of grains and the clast, presumably the result of increasing iron content (Fig. 8B). Clast dolomite fluoresces red under CL, the result of the activation of trace Mn^{2+}; quenching (brown to nonluminescing) is due to Fe^{2+} (Machel, 1985). Matrix dolomite does not fluoresce, or only shows very weak fluorescence under CL (Fig. 8B).

Massive magnetite-dolomite carbonatite contains veinlets which are <1 mm in diameter and are typically surrounded by a thin halo devoid of opaque minerals that appears bleached at hand-sample scale (Fig. 6B). The veinlets are composed of fresh fine-medium-grained barite and dolomite (Fig. 9). The groundmass in this sub-unit is uniformly very fine-grained and contains only a few millimeter-sized dolomite clasts.

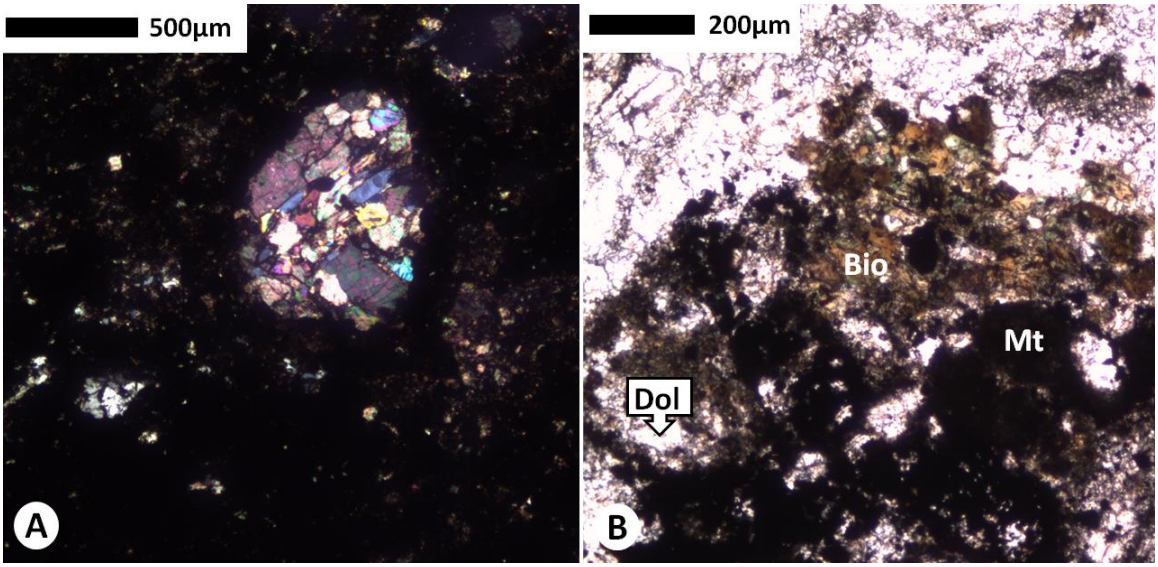

Fig. 7: (A) Cross-polarized light image of a rounded clast of dolomite carbonatite surrounded by fine-medium grained magnetite-dolomite carbonatite matrix (EC-29 1490'). (B) Plane-polarized light image of biotite in magnetite-dolomite carbonatite. These grains are typically found near the margins of dolomite-carbonatite clasts. Anhedral dolomite grains visible in magnetite-dolomite matrix (bottom of image) (EC-11 2422').

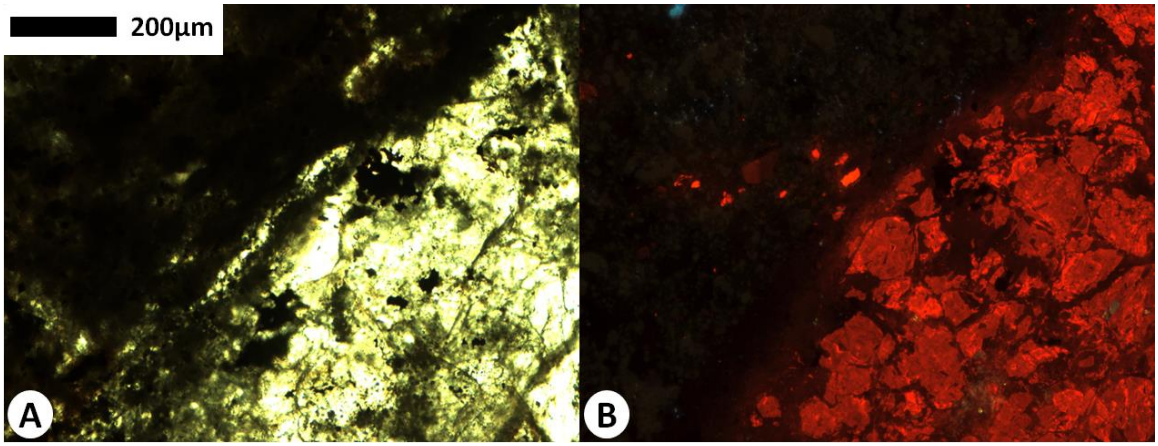

Fig. 8: The outer margin of a dolomite clast in a magnetite-dolomite carbonatite matrix. Matrix consists mostly of opaque minerals. Dolomite grains show partial quenching (brown to

nonluminescing) at grain boundaries inside clast and on the rim of the clast (A) plane-polarized light and (B) cathodoluminescence (EC-16 2410')

Very dense massive magnetite-dolomite carbonatite occurs as nearly-black pods and localized zones in magnetite-dolomite carbonatite and as rare fragments in dolomite carbonatite breccia (Fig. 6B). These intercepts are narrow (typically less than 3-meter-long core intercepts) and the rock is strongly magnetic. The rock is uniformly very fine-grained and magnetite appears to be the dominant rock-forming mineral in these intervals (Fig. 10).

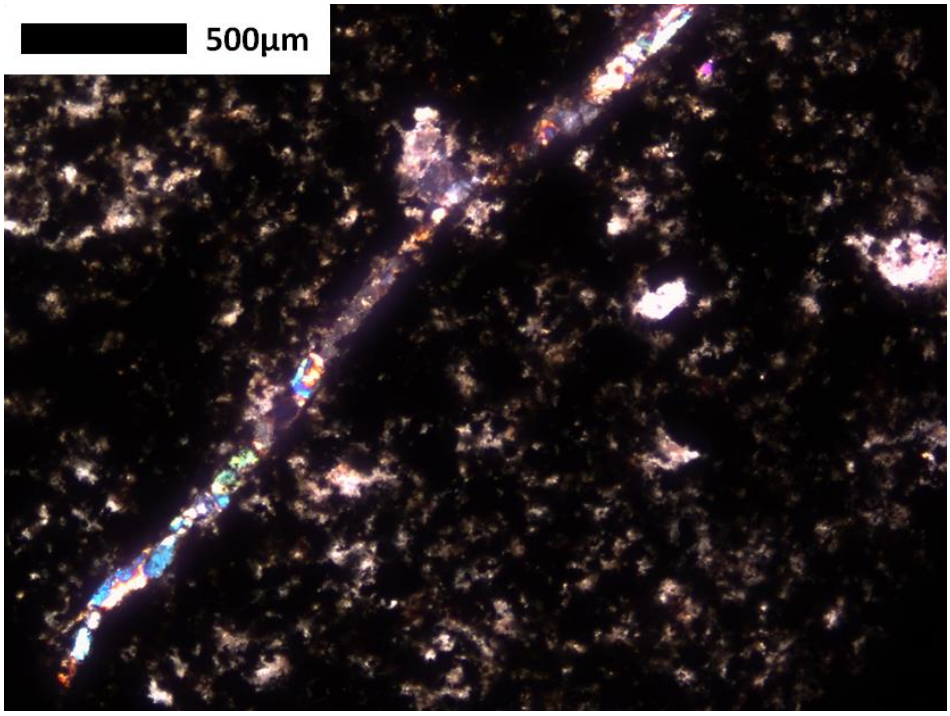

Fig. 9: Cross-polarized light image of barite veinlet cutting across magnetite-dolomite carbonatite (EC-28 1975').

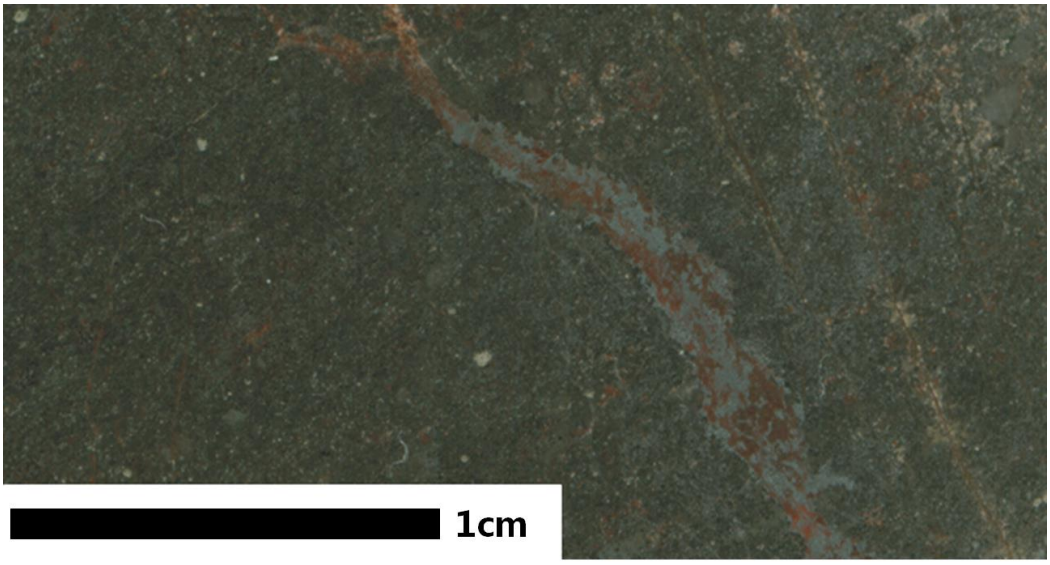

Fig. 10: Thin section scan (reflected light) of massive, magnetite-rich magnetite-dolomite carbonatite with a barite-hematite veinlet at center-right (EC-28 1975.5').

Although much of the massive magnetite-dolomite carbonatite rock contains abundant magnetite, some rocks classified as magnetite-dolomite carbonatite contain less than 10% fine-grained disseminated magnetite + ilmenite. These rocks are only weakly magnetic. In thin-section, these rocks have a "salt and pepper" appearance with disseminated fine-grained opaque minerals (Fig. 11). Fine-grained dolomite and fine-to-medium-grained barite are the primary rock-forming minerals in this sub-unit. Veinlets are abundant, and are typically surrounded by a light-colored halo that is wide relative to the size of the veinlet (Fig. 11). Secondary hematite and limonite dusting is also more pervasive in these rocks.

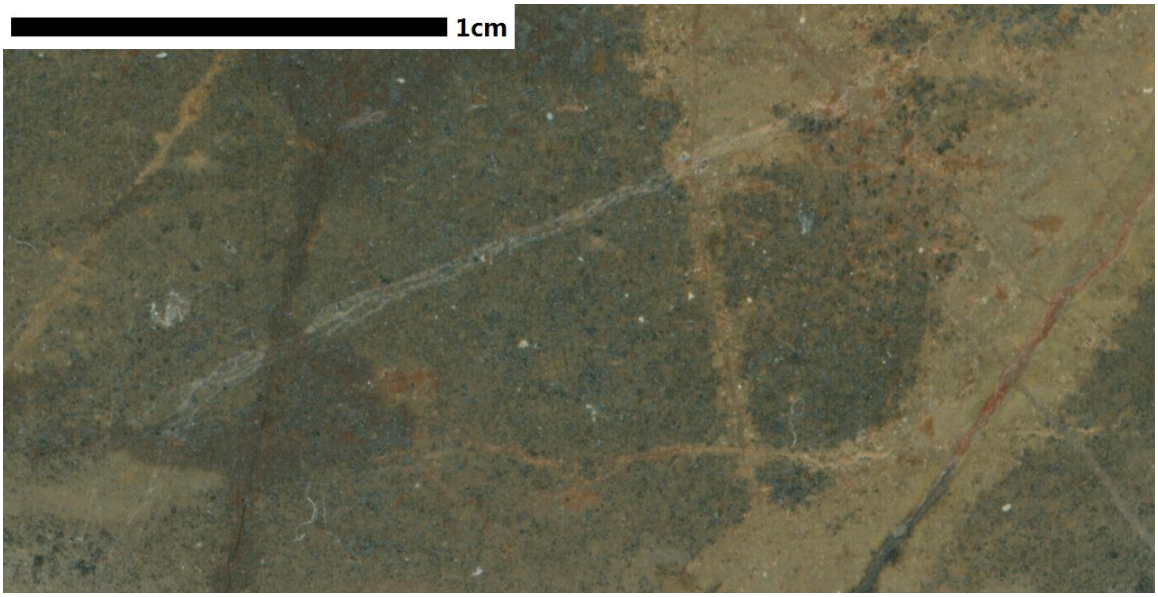

Fig. 11: Thin section scan (reflected light) of massive magnetite-dolomite carbonatite with barite-hematite veinlets. Darker matrix contains disseminated fine-grained magnetite and ilmenite, with patches of hematite/limonite alteration and pervasive minor hematite dusting. Veinlet halo is fine-grained dolomite and barite (EC-29 1392').

Barite is an abundant mineral in the magnetite-dolomite carbonatite, and occurs in microveinlets along with hematite and dolomite (Figs. 9-11) and as aggregates and disseminations in the magnetite-dolomite carbonatite matrix. These barite grains appear fresh and are unzoned euhedra-subhedra under backscattered electron imaging (Fig. 12). Sulfides (pyrite, rarely chalcopyrite) are found as disseminations, patches, and as clusters of thin stringers and veinlets in magnetite-dolomite carbonatite. Individual grains are most commonly brass-colored pyrite and appear to be fresh.

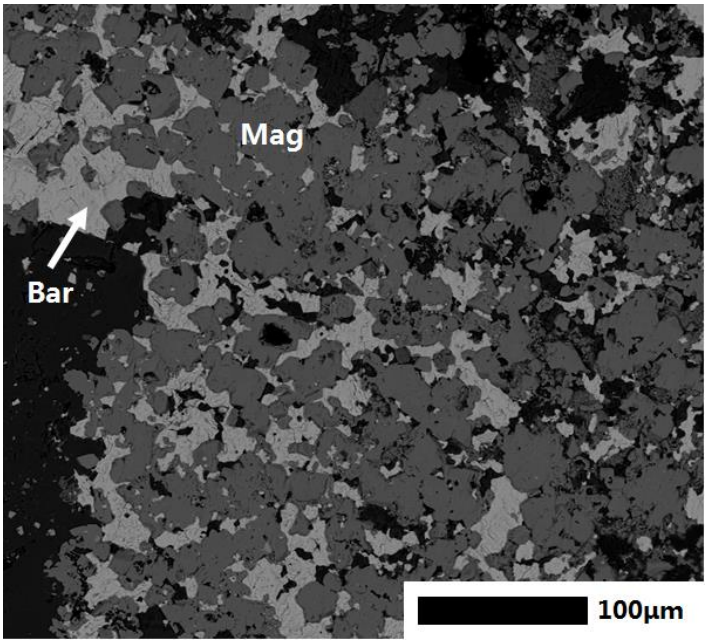

Fig. 12: Backscattered electron image of abundant barite in magnetite-dolomite carbonatite (EC11-2422')

A brecciated variant of magnetite-dolomite carbonatite is also present in core intercepts (Fig. 6C). Small (1-20 mm long) angular-subangular fragments of dolomite carbonatite are surrounded by a matrix of magnetite-rich dolomite-carbonatite rock. The matrix is fine-grained, strongly magnetic, and a uniform dark grey color. The boundaries between dolomite clasts and the magnetite-rich matrix in this sub-unit are not sharp and are similar in appearance to Fig. 7B.

The contacts between magnetite-dolomite carbonatite and surrounding rocks are often obscured by pervasive alteration, but typically the boundary is defined by a gradational transition from solid magnetite-dolomite carbonatite to a dolomite carbonatite breccia with clasts of magnetite-dolomite carbonatite (Fig. 13). Sharp contacts with

dolomite carbonatite are marked by apparent bleaching of the magnetite-dolomite carbonatite when viewed in hand sample.

The physical properties of the magnetite-dolomite carbonatite rock are somewhat different in comparison to the other carbonatite and silicate rocks in the ECCC. The magnetite-dolomite carbonatite is denser than the other lithologic units (Drenth, 2014). The mean density of magnetite-dolomite carbonatite is 3200 kg/m^3, whereas all other carbonatite rocks in the ECCC have mean densities between 2800 and 2910 kg/m^3 (Drenth, 2014). Qualitatively, the massive magnetite-rich variety (Fig. 6B) has the highest density. Mean magnetic susceptibility for the magnetite-dolomite carbonatite is two to three orders of magnitude higher than the other carbonatite rock units in the complex (Drenth, 2014). Unaltered hand samples will easily attract magnets; this property is most pronounced in the dark massive magnetite-dolomite carbonatite.

4.1.4 Dolomite Carbonatite Breccia: This rock type (Molycorp: Beforsite Breccia) comprises clasts of dolomite carbonatite, magnetite-dolomite carbonatite, and mafic dike rock in a matrix of fine-grained dolomite carbonatite. Clasts of magnetite-dolomite carbonatite 1-20 cm long occur as fragments in dolomite carbonatite breccia (Sherer, 1981). The edges of the clasts are relatively sharp with a local small alteration rind on the magnetite-rich side.

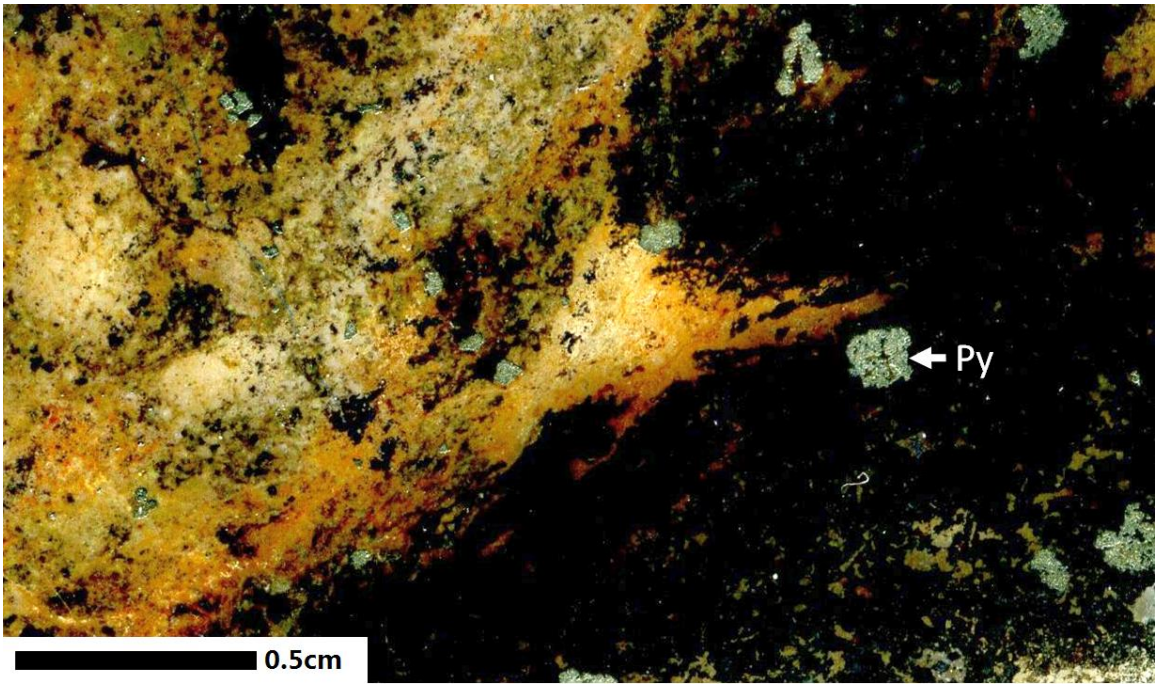

Fig. 13: Thin section scan (reflected light) of altered dolomite carbonatite breccia (left) with a dark magnetite-dolomite carbonatite clast (right). Light-colored matrix (left) consists of fine-grained dolomite, barite, apatite, and hematite. Large disseminated grains with metallic luster are identified as pyrite (EC-30 1074')

These clasts tend to be heavily veinleted, and have reaction rims at the inner margins of the clast. In unaltered breccia, clasts of magnetite-dolomite carbonatite are ferromagnetic; on the other hand, magnets are not attracted to either altered clasts or matrix material. Both varieties of magnetite-dolomite carbonatite are represented as clasts in this breccia unit. Veinlets inside magnetite-dolomite carbonatite clasts are typically very fine-grained, thin (<1 mm), white-light grey, and react weakly to HCl. They are typically surrounded by a small envelope of bleaching. The niobium grade of the whole-rock is controlled by the occurrence of magnetite-dolomite clasts relative to the matrix. Some core is

pervasively altered to friable and porous earthy yellow-red rock, and original texture can only be seen in thin-sections derived from more competent zones (Fig. 14).

4.1.5 Oxidized Dolomite Carbonatite: Oxidized dolomite carbonatite rock is a common feature in the Elk Creek Carbonatite Complex, and intercepts with pervasive iron oxidation can be tens of meters long in core. The style of this mineralization ranges from veinlet-hosted (Fig. 10) to pervasive (Fig. 14), with both hematite and limonite occurring as oxidized iron minerals. Pervasively-oxidized dolomite carbonatite is typically friable and brittle, especially when limonite is the dominant oxidation mineral as in Fig. 14.

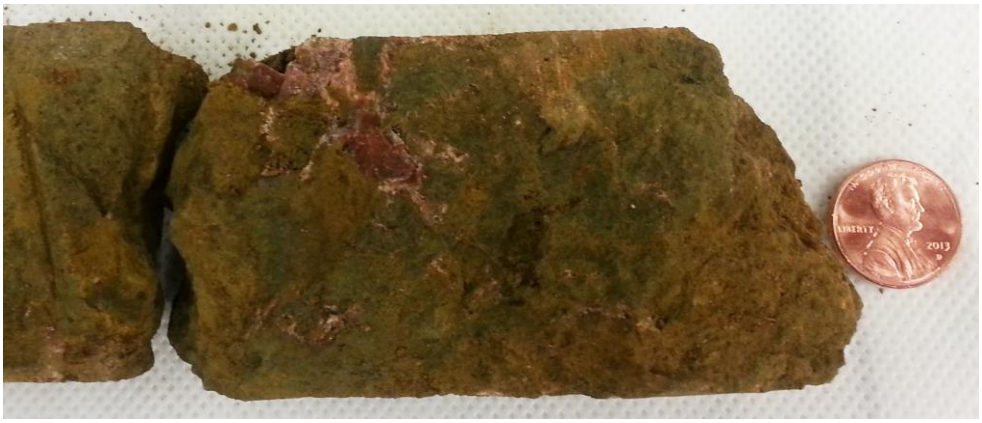

Fig. 14: Hand-sample image of pervasively hematite-limonite-altered dolomite carbonatite breccia. Large pink-red bladed barite crystals (center-left) occur as veinlets and vug/fracture fill; these barite veinlets cut across both clast rock and matrix (EC-26 1954').

4.1.6. Barite-Dolomite Carbonatite: Barite-rich, REE-mineralized dolomite carbonatite rock (Molycorp: Barite Beforsite) was not intercepted in the niobium ore zone with the exception of <10 cm veinlets. These veinlets are pink-white, fine-grained, and

are composed of a mixture of dolomite and barite with accessory apatite. These veinlets and vugs can contain prismatic barite blades up to 10 cm long (similar to Fig. 14) with microcrystalline dolomite, hematite, and apatite as secondary fill. The dolomite is frequently microcrystalline and has a milky appearance in hand sample; barite-dolomite carbonatite dikes containing this variety of dolomite have a vuggy texture with barite, pyrite, and fluorite infilling open cavities.

Massive pink-white barite-dolomite carbonatite does not appear in the niobium ore zone. In thin-section, anhedral dolomite and barite are the major rock-forming minerals in massive barite-dolomite carbonatite, with hematite and fine-grained REE minerals occurring as vug and fracture-fill minerals. Zones of pristine dolomite carbonatite are surrounded by cloudy rims with barite, dolomite, apatite, and quartz occurring outside these zones (Fig. 15A). Rare-earth fluorocarbonate minerals form patches of acicular crystals in this alteration zone, sometimes occurring with purple fluorite (Fig. 15B). REE-host minerals include monazite, xenotime, bastnaesite, and parisite based on microprobe analysis and EDS spectra.

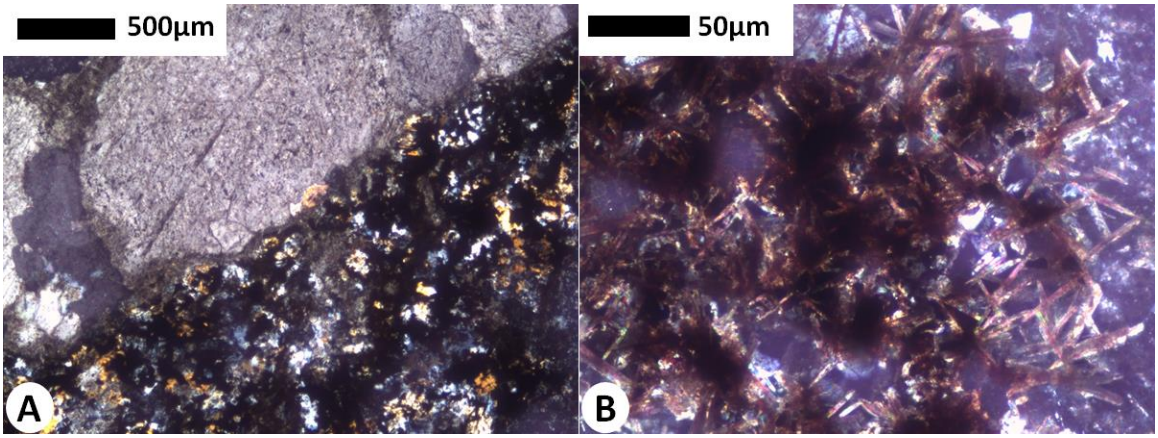

Fig. 15: Cross-polarized light images of (A) Euhedral dolomite in barite-dolomite carbonatite (top left) surrounded by opaque minerals, barite, quartz, and secondary dolomite. Cloudy clast rims are similar to altered dolomite in Fig. 15 (EC-43 812'). (B) Acicular blades of REE fluorocarbonate minerals in the alteration zone with patches of very fine-grained barite and fluorite (EC-43 812').

4.1.7 Syenite: Syenite (Molycorp: Syenite I, II) was intercepted in core at the periphery of the ECCC but is not present in the main niobium ore zone. These rocks contain primary orthoclase and biotite, and have been significantly overprinted with secondary dolomite (Xu, 1996). Molycorp logs report the presence of nepheline, sanidine, phlogopite, muscovite, and zircon (Sherer, 1983a). The syenites do not contain niobium pyrochlore as an accessory mineral. Molycorp geologic logs and reports from borehole EC-4 indicate that the syenite was emplaced relatively early in the formation of the Elk Creek complex; dolomite carbonatite dikes, lamprophyres, and mafic dikes cut across the syenite (Sherer, 1983a).

4.1.8 Mafic Dike: Small mafic dikes (typically <3 m thick in core intercepts) are seen throughout the Elk Creek carbonatite (Molycorp: Older Mafic). These dikes have

high magnetic susceptibility when unaltered but have low background levels of niobium mineralization (≤0.1% Nb_2O_5). The texture is very-fine-grained, massive to slightly porphyritic or flow-banded, with a dark grey-green color (Fig. 16A). Porphyritic mafic veins contain small rounded white phenocrysts comprised of dolomite, proposed to be a replacement of olivine and pyroxene (Xu, 1996). Mafic dikes will frequently effervesce when HCl is applied, indicating the presence of abundant dolomite. Contacts with carbonatite rocks are sharp or undulatory with up to 10 cm of alteration on both sides of the contact. These dikes have sharp intrusive contacts with the magnetite-dolomite carbonatite, but occur as xenoliths within later carbonatite units (Sherer, 1981). Massive dolomite carbonatite contains this unit as xenoliths but is also cut by dikes of this lithology (Xu, 1996). Dolomite carbonatite breccia contains fragments of this mafic rock; the clasts are typically rounded and centimeter-scale in diameter (Sherer, 1981).

4.1.9 Lamprophyre: The complex is also cut by silicate dikes possessing visible euhedral biotite grains (Molycorp: Younger Mafic). This rock is not magnetic and does not contain significant niobium. The texture is porphyritic, with coarse-grained biotite in a matrix of fine-grained grey-green rock (Fig. 16B). These biotite phenocrysts can be as large as 3 cm in longest dimension. Biotite grains are locally parallel along preferred orientation planes when observed in core, but these lineations are typically absent as in Fig. 16B. The groundmass is composed of biotite, orthoclase, opaque minerals, and dolomite (Xu, 1996). This mafic unit also contains rare cm-scale xenoliths of medium-to-coarse-grained crystalline dolomite carbonatite. Contacts with carbonatite rocks are typically sharp or undulatory, and these dikes cut through nearly all other lithologic units

in the ECCC. They are, however, recorded as both veins and xenoliths in barite-dolomite carbonatite and dolomite carbonatite breccia (Sherer, 1981).

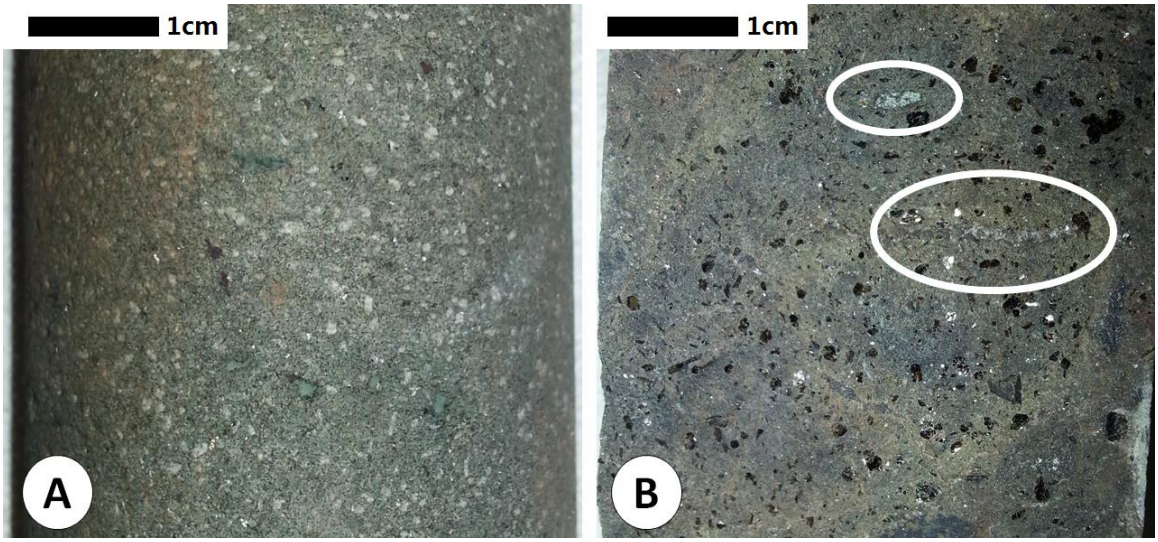

Fig. 16: Hand-sample images of (A) Fine-medium-grained mafic dike with white phenocrysts (EC-4 1920') (B) Porphyritic lamprophyre with abundant biotite crystals in a fine-grained matrix. Contains sparse elongate clasts of dolomite carbonatite (circled) (EC-26 2273').

4.1.10 Cross-cutting Lithological Relationships: Few pristine contacts exist between the magnetite-dolomite carbonatite (MDC) and the other carbonatite units at Elk Creek, but some conclusions on the paragenetic order of the MDC can be drawn from unaltered contacts reported by Molycorp in core and confirmed by follow-up examination in the course of this work (Fig. 17). The MDC is older than the massive apatite-bearing dolomite carbonatite, both the coarse-grained and medium-fine-grained variety. A cm-scale alteration halo is observed on the MDC side, and porphyroclasts and internal veinleting are truncated by contacts. The MDC is also cut by both varieties of mafic rock, and appears as clasts in dolomite carbonatite breccia. This would suggest that the MDC

was intruded early in the formation of the carbonatite complex. However, the porphyritic/microbrecciated texture of the MDC suggests a pre-existing dolomite carbonatite rock was in place before the intrusion of the reduced iron-rich melt. Differences in pyrochlore chemistry between conjugate clast pyrochlore (Type 2) and matrix pyrochlore (Type 3) indicate different pulses, with Type 2 grains being accessory minerals in the pre-existing dolomite carbonatite. The fresh appearance of barite and pyrite in magnetite-dolomite carbonatite, as well as cross-cutting relationships to other minerals suggest that these were the result of later-stage fluids.

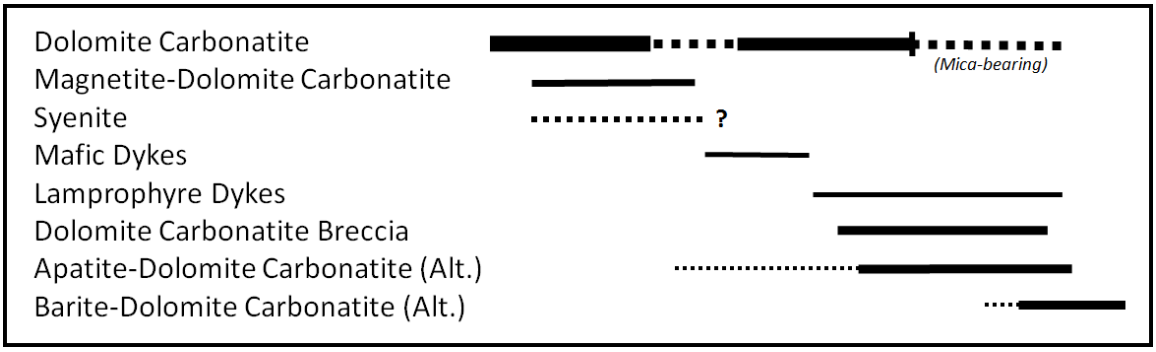

Fig. 17: Proposed genetic order interpretation for carbonatite and silicate lithologies in the Elk Creek Carbonatite Complex based on unit contacts observed in drill cores, petrography, and Molycorp geological logs. Line thickness represents relative volumetric abundance in the carbonatite complex.

Mafic dikes appear fairly early in the complex, cutting across magnetite-dolomite carbonatite but appearing as xenoliths and clasts in all other rock types. Lamprophyre dikes are the latest discernable pulse of silicate magma in the Elk Creek system. Sherer (1984b) reported that some intercepts of barite-dolomite carbonatite contain xenoliths of lamprophyre, indicating carbonatite magma injection occurred during or after

lamprophyre emplacement. Molycorp work also indicates that the biotite-bearing variant of dolomite carbonatite cuts across massive dolomite carbonatite but is older than barite-dolomite carbonatite (Sherer, 1984b) After this point, the brecciation of large zones within the carbonatite body occurred; the dolomite carbonatite breccia contains clasts of all lithologic units and is only rarely cut by late lamprophyre dikes. This is the last apparent major injection of carbonatite melt into the complex.

4.2 Niobium Mineralization

4.2.1 Pyrochlore: The primary contributor to the overall budget of niobium mineralization in the Elk Creek Carbonatite is niobium pyrochlore, with an additional minor contribution from niobian rutile and ilmenite. Other niobium ore minerals such as columbite and perovskite-group minerals were not observed in thin-section or by EDS/microprobe XRF analysis. This is consistent with earlier Molycorp work, which did not report alternative major niobium mineral phases (Mariano, 1978). Classification of pyrochlore types is based on differences in chemistry, morphology, and host rock. Historical classifications from Molycorp workers are presented for reference where applicable (Mariano, 1978).

Type 1 pyrochlore (Molycorp: Generation 1) is uncommon outside of rare 1-10 meter intercepts of mineralized dolomite carbonatite. These pyrochlores are euhedral, with a size of 100 μm to 2 mm in longest dimension (Fig. 18). These grains can be seen at hand-lens scale as pale white-yellow octahedra disseminated in carbonatite. When observed in transmitted light, they are typically pale yellow with deeper color in the core, relatively sharp color zones, and numerous small inclusions (Fig. 18).

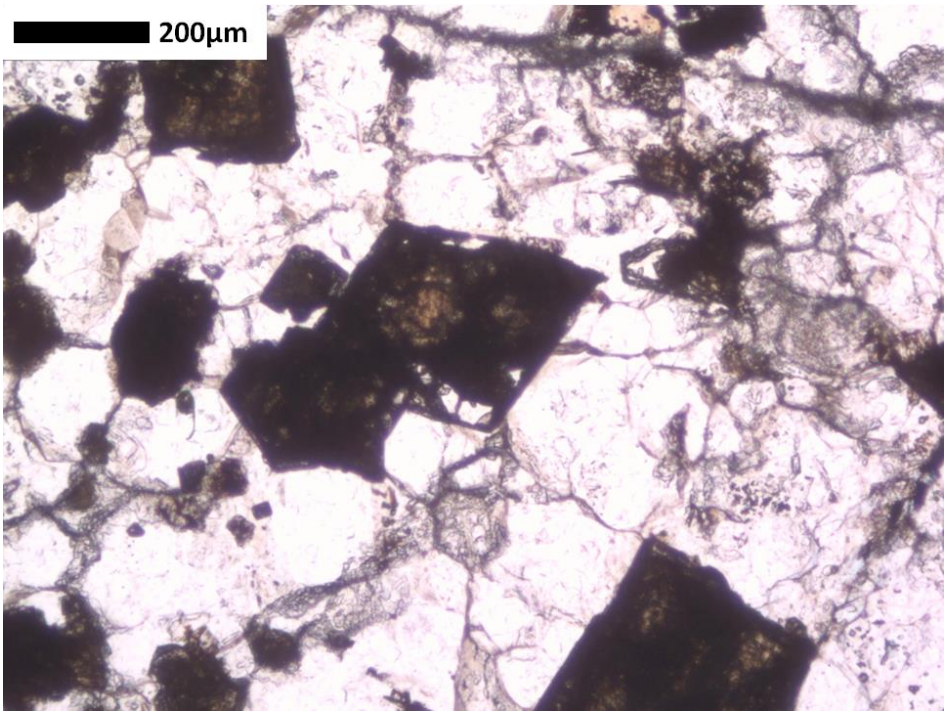

Fig. 18: Plane-polarized light image of Type 1 pyrochlore grains in dolomite carbonatite. Some grains are partially skeletonized. Smaller pyrochlores visible at center-left as inclusions in dolomite (EC-15 849').

Oscillatory zoning is seen in most instances and zoned rims/cores are also common when Type 1 pyrochlore grains are viewed in backscattered electron images (Fig. 19). Grains also exhibit a "pitted" appearance, with voids occurring inside euhedra (Fig. 18). These voids cut across zones but some zones contain more pits relative to others. This type of pyrochlore is observed principally as a primary accessory mineral in dolomite carbonatite. Additionally, Molycorp workers identified and reported rare fragments of large amber-colored pyrochlore with concentric zoning in magnetite-dolomite carbonatite and in the matrix of the dolomite carbonatite breccia in drill hole

EC-29 (Sherer, 1983b). This description matches the criteria for Type 1 pyrochlore, but is not yet confirmed by chemistry.

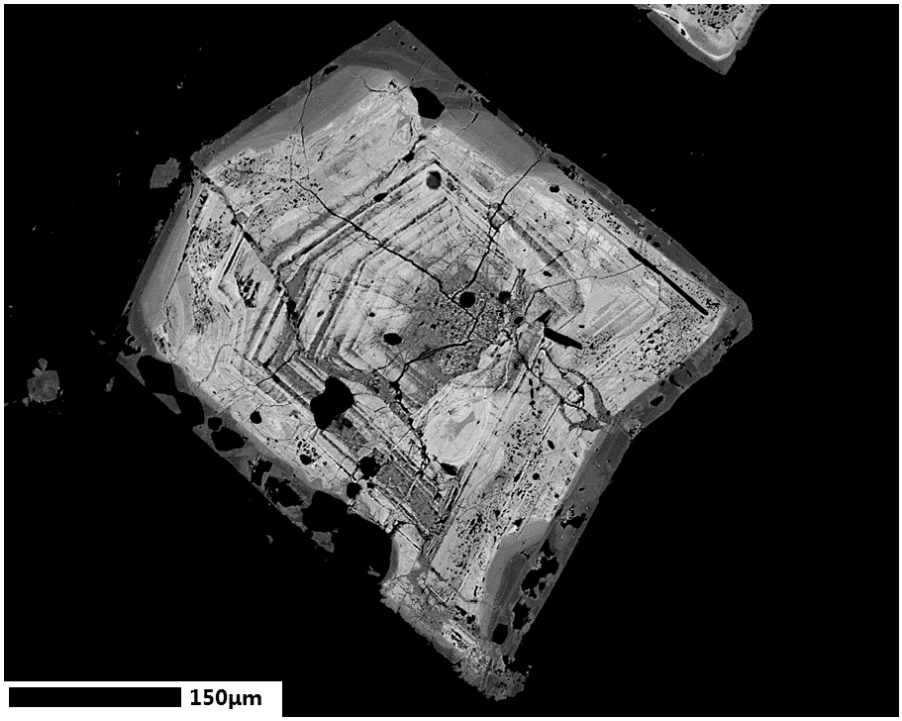

Fig. 19: SEM backscatter image of Type 1 pyrochlore with concentric zoning. Bright zones contain 5-10% Ta_2O_5, dark zones contain 0-1% Ta_2O_5 with a subsequent increase in Nb_2O_5 (EC-15 849').

Type 2 pyrochlore (Molycorp: Generation 2 and 3) occurs in nearly all carbonatite lithologies at Elk Creek, although typically as a very minor accessory mineral composing 0.2% or less of mineralogy by modal volume. These grains appear as euhedral inclusions in dolomite and apatite, as well as grains interstitial to other rock-forming minerals (Fig. 20A). Typically, Type 2 pyrochlores are 10-100 µm in longest dimension, euhedral, and are transparent to cloudy grey under transmitted light (Fig. 20B). A few of these

pyrochlores are weakly zoned, but most are uniform with minor inclusions (Fig. 21). Pits and voids are observed but most grains have solid, sharp, and continuous boundaries.

Like Type 1 pyrochlores, these pyrochlores are also seen in <10 m intercepts of mineralized dolomite carbonatite as a significant accessory mineral in localized zones (1-3% modal volume). In these zones, pyrochlore grains occur as disseminations and in mineralized bands within and around dolomite and apatite anhedra (Fig. 20A). Most grains are single euhedra, but a small percentage occur as clusters of 2-5 grains. Distribution of these pyrochlores is patchy and uneven. In a thin section from a localized high-grade niobium intercept in dolomite carbonatite (EC-43 1069'), the abundance of pyrochlore grains progresses from almost totally absent to 10% pyrochlore by modal volume over the length of a standard 1x2" thin section. The pyrochlore "clusters" also contain opaque minerals and a higher degree of hematite dusting/alteration, whereas the barren rock is nearly pure dolomite. In barite-dolomite carbonatite, rare pyrochlore occurs as euhedral inclusions in dolomite, similar to unaltered dolomite carbonatite; these grains are not observed in the barite-dominated alteration zones. Type 2 pyrochlore grains are also found in the dolomite carbonatite clasts in magnetite-dolomite carbonatite, but are not evenly distributed. A few clasts contain a dense concentration of 10-100 μm pyrochlore grains occurring in bands and as disseminated inclusions in dolomite (similar to Fig. 20A), but more commonly the clasts only contain a few grains or are unmineralized.

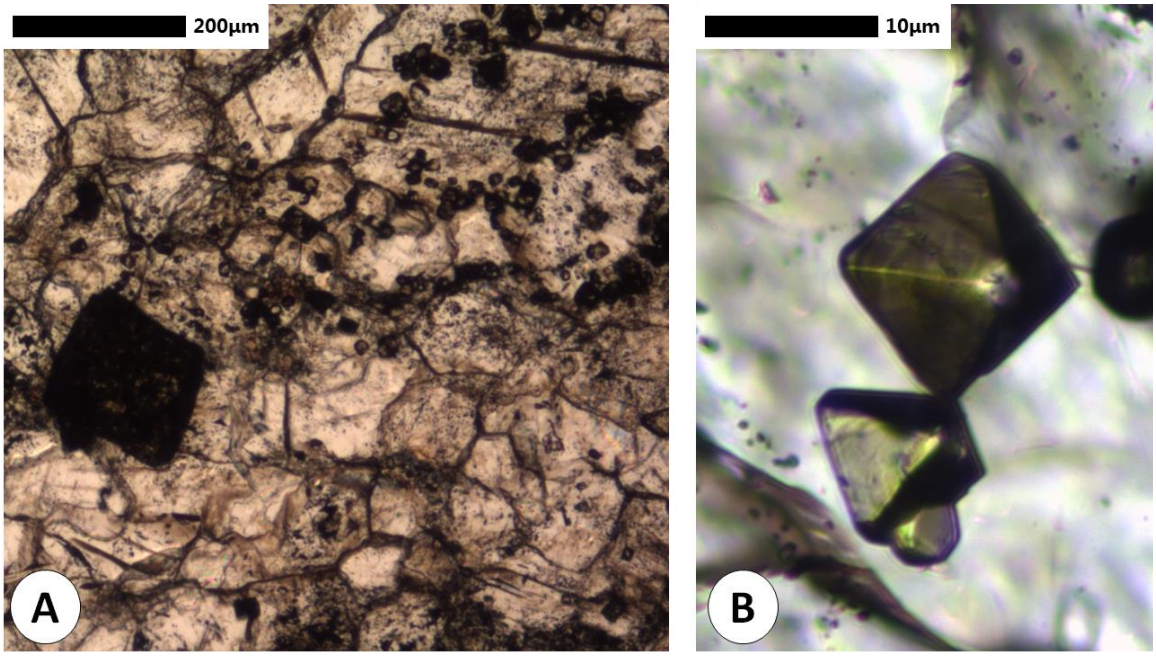

Fig. 20: (A) Plane-polarized light image of Type 2 pyrochlore grains in dolomite carbonatite. Rare grains are larger than 100 µm in longest dimension, as seen at middle-left. (EC-43 1043'). (B) Cross-polarized light image of Type 2 pyrochlore euhedra (EC-43 1043')

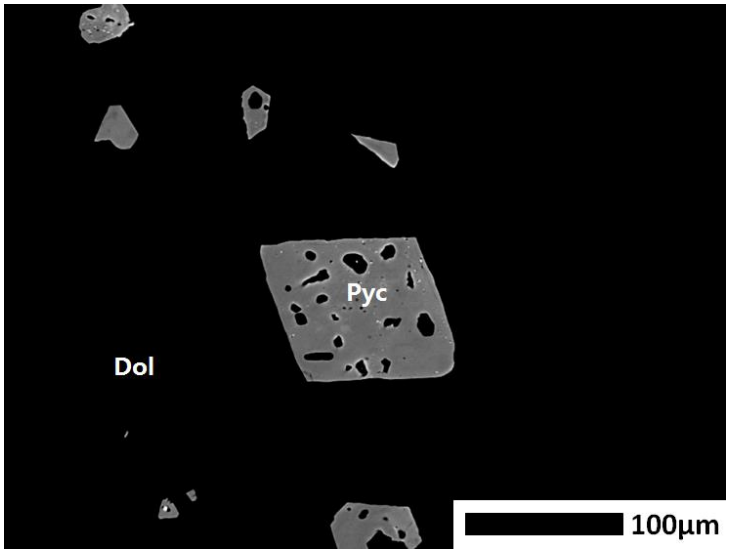

Fig. 21: SEM backscatter image of Type 2 pyrochlore grains in dolomite carbonatite (EC-43 1069')

Type 3 pyrochlore is limited to the magnetite-dolomite carbonatite and is the principal contributor to the consistently high niobium grade in these rocks. These pyrochlore grains are very small, rarely exceeding 10 μm in longest dimension, and occur as subhedral inclusions in magnetite (Fig. 22A) and anhedral inclusions in ilmenite (Fig. 22B). Type 3 grains also occur in patches of euhedral to subhedral grains disseminated in the magnetite-bearing matrix (Fig. 23), and as inclusions in dolomite. These patches can feature densely-packed pyrochlore euhedra in localized <1mm areas, resembling slightly disrupted aggregates (Fig. 23). Pyrochlore inclusions are more common and more pervasive in ilmenite than in magnetite. Significant variation was observed with respect to pyrochlore inclusions in magnetite – many contained no pyrochlore at all, especially small (<100 μm diameter) euhedral magnetite grains. However, most medium and large magnetite crystals contain at least a few pyrochlore inclusions, and a small number are densely-packed with pyrochlore inclusions. A few small grains are seen under electron microscopy to have gradational boundaries with neighboring magnetite and ilmenite, but typical contacts are sharp and continuous laterally with no gaps or alteration rims (Fig. 22B). These pyrochlores are unzoned and appear to have uniform composition under backscattered electron imaging. Type 3 pyrochlore inclusions are not visible in transmitted light; backscattered electron imaging was relied upon to characterize their morphology.

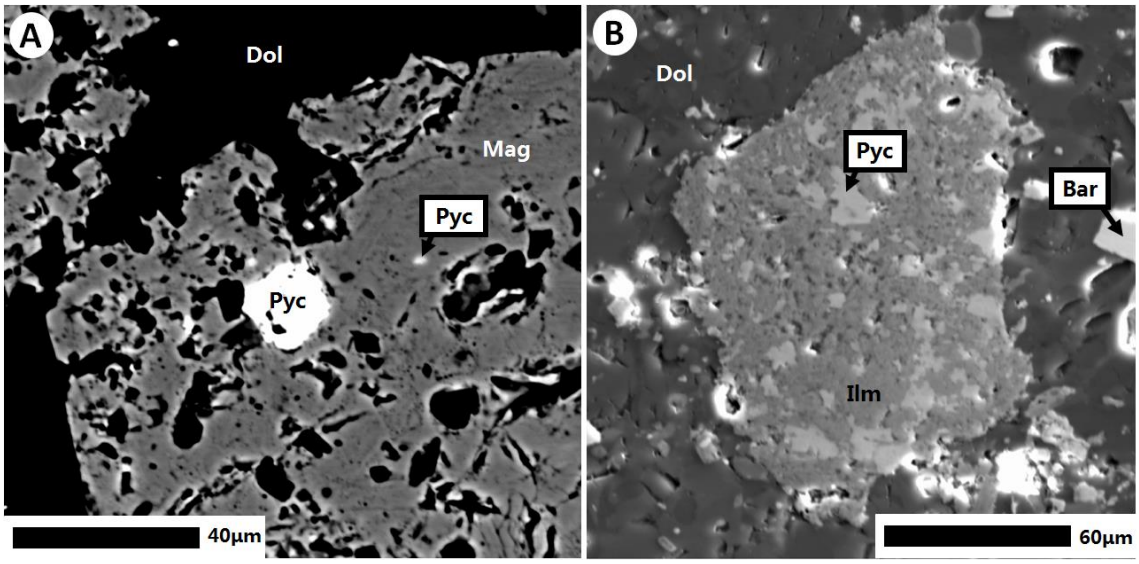

Fig. 22: (A) SEM backscatter image of pyrochlore grains in partially-altered magnetite. Type 3 pyrochlore grains are typically 5-10 µm (but can be <1 µm) in longest dimension (EC-29 1392). (B) Secondary electron imaging of abundant Type 3 pyrochlore grains in ilmenite (EC-29 1147')

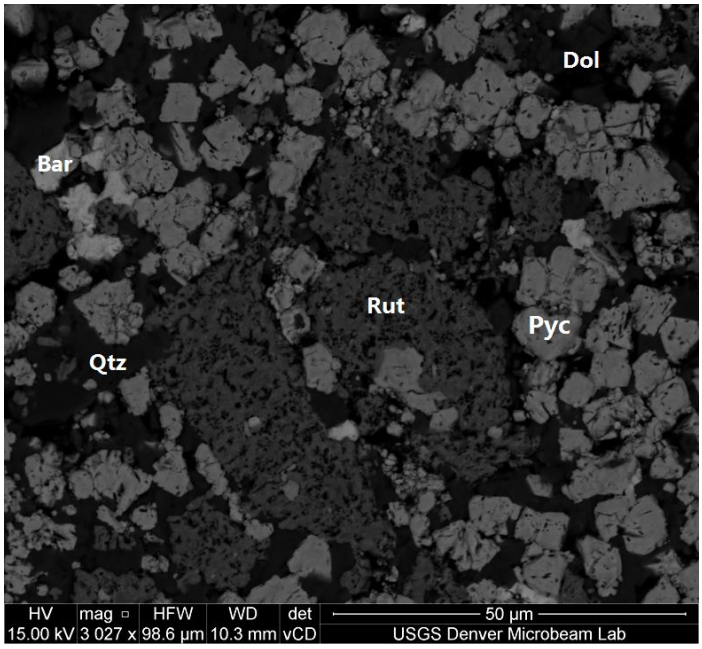

Fig. 23: SEM backscatter image of euhedral-subhedral Type 3 pyrochlore grains in an aggregate cluster consisting of pyrochlore, rutile, barite, dolomite, and quartz (EC-11 2422').

A potential fourth type of niobium pyrochlore is reported by Molycorp workers in internal reports. Energy-dispersive spectral analysis performed by Molycorp found pyrochlores with major barium substitution in massive barite-dolomite carbonatite in borehole EC-48 (Sherer, 1984c). This drill hole is outside of the main niobium ore zone and was not evaluated for this report, but the Molycorp report for borehole EC-48 presents EDS spectra showing barium substitution (Sherer, 1984c). Strongly barium-enriched pyrochlore grains were not observed in this study.

4.3.2 Secondary Niobium Minerals and Including Minerals: Prior Molycorp work referenced in passing that niobian rutile is present in the ECCC; further examination is reasonable for this study (Mariano, 1978). Rutile occurs as an accessory mineral in some intervals of magnetite-dolomite carbonatite. Typically this mineral is found in contact

with and contained within grains of ilmenite and pyrochlore (Fig. 24). Individual grains are small (<100 μm and often less than 30 μm in longest dimension) and are in continuous contact with surrounding pyrochlore and ilmenite. Pyrochlore inclusions in rutile are much less common than pyrochlore inclusions in ilmenite (Fig. 24).

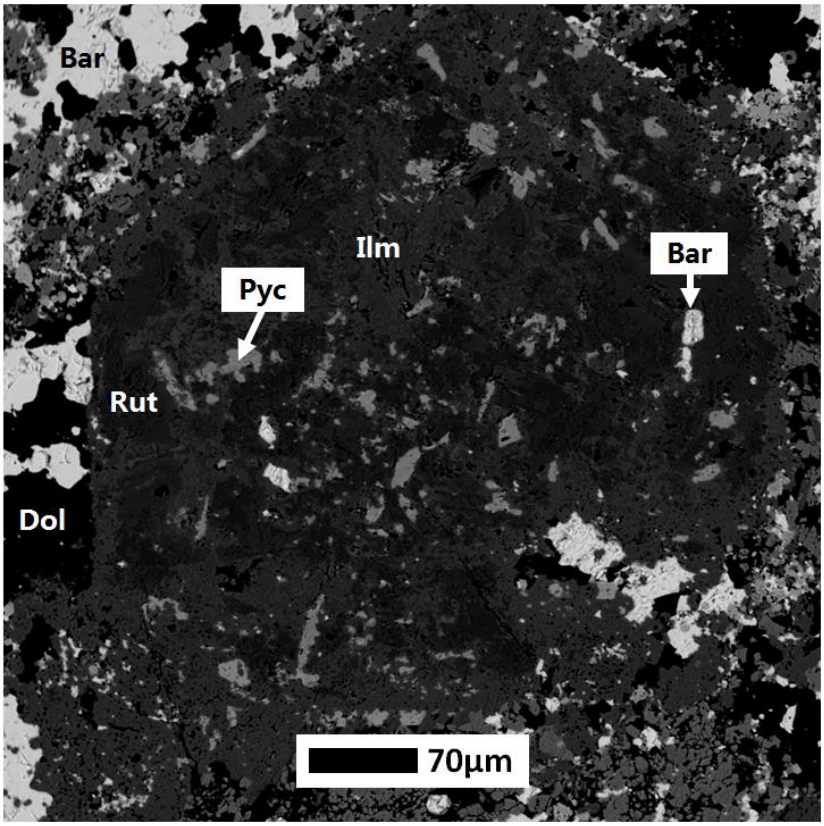

Fig. 24: SEM backscatter image of large ilmenite-rutile grain in a magnetite-dolomite carbonatite clast with Type 3 pyrochlore inclusions. Ilmenite is slightly brighter under backscattered electrons compared with rutile. Ilmenite predominates at rim, but distribution inside grain is chaotic (EC-30 1074').

Ilmenite occurs as single grains and aggregates up to 500 μm diameter with internal pits and voids (Fig. 22B). The rims of ilmenite grains tend to have a jagged

appearance with embayments containing dolomite and barite crystals. Magnetite has an even more skeletal appearance but the outlines of original magnetite euhedra are apparent (Fig. 22A). None of these minerals appear zoned in backscattered electron imaging.

5. Magnetite-dolomite Carbonatite: Unusual Whole-rock and HFSE Geochemistry

As suggested by the name, the most notable geochemical aspect of the magnetite-dolomite carbonatite is strong enrichment in iron. This enrichment is variable, ranging from 12.7 to 21.7% FeO, and corresponds to high niobium grades (0.85 to 1.49% Nb_2O_5) (Table A1). The magnetite-dolomite carbonatite is also enriched in Ti compared to other carbonatite rocks at Elk Creek (Table 1), and has a higher SiO_2 concentration (Table A1). Phosphorous is depleted in the magnetite-dolomite carbonatite relative to other units, and corresponds to the paucity of apatite seen in thin-section. Some notable trace-element characteristics of the magnetite-dolomite carbonatite are enrichment in W, Th, and Zn relative to other carbonatite rocks in the complex (Table A1).

Niobium grades in magnetite-dolomite carbonatite are consistently high, with observed concentrations of 0.6-1.04% elemental niobium (0.85-1.49% Nb_2O_5) (Table 1). Other carbonatite lithologies in the ECCC have typical niobium concentrations of 500-1000 ppm elemental Nb, whereas mineralized intervals of dolomite carbonatite have concentrations of 6000 ppm or higher (Table 1). Niobium grades in the silicate rocks (mafic dikes, syenites) are below 1000 ppm Nb (Table 1). This agrees well with typical grades obtained by Molycorp from their initial exploratory drilling and analysis (Mariano, 1978). With respect to other HFSEs, the magnetite-dolomite carbonatite is less

unusual; Ta, Zr, and Hf concentrations are comparable to other carbonatite rocks in the complex.

Table 1: HFSE geochemistry in parts per million for selected representative Elk Creek carbonatite samples compared to average carbonatite values compiled by Chakhmouradian (2006).

Lithology (Borehole)	**Nb**	**Ta**	**Zr**	**Hf**	**Ti (%)**	**Nb/Ta**	**Zr/Hf**
Magnetite-dolomite carbonatite (EC-29 1480’)	10400	26.2	48.5	2	0.36	396	24.3
Magnetite-dolomite carbonatite (EC-11 2425')	8400	6.5	95	5	3.12	1292	19
Magnetite-dolomite carbonatite (EC-16 1380')	5970	12	99.8	4	1.74	497	25
Dolomite carbonatite (EC-15 1010')	620	20.1	17.9	<1	0.16	31	17.9
Dolomite carbonatite, Nb-mineralized (EC-43 1060')	6870	8.1	88.6	2	0.13	848	44.3
Barite-dolomite carbonatite (EC-4 1225')	913	0.2	71.5	1	0.2	4565	71.5
Lamprophyre (EC-20 1210')	952	10.3	397	8	1.71	92	50
Syenite (EC-82 970')	377	7.3	13.3	11	1.02	52	1
Averages compiled by Chakhmouradian, 2006							
Phoscorites	557.2[1]	32	729.1[2]	12.8	1.83	17	57
Magnesiocarbonatites	255.4	8.1	248.4	4.1	0.23	32	61
Ferrocarbonatites	252.4	9.3	146.2	1.6	0.33	27	91
All carbonatites	308.9	8.9	256.4	4.3	0.28	35	46
Kola alkali-ultramafic intrusions	95.8	5.5	347	7.6	2.68	17	60

[1]Range from 12 to 12237 ppm
[2]Range from 16 to 5410 ppm

A second notable difference between the magnetite-dolomite carbonatite and the other units in the ECCC is the distribution of rare-earth elements (Fig. 25). The other lithologies in the ECCC follow the typical carbonatite trend of strong LREE enrichment

with a steep downward slope towards the heaviest rare-earth elements (Hornig-Kjarsgaard, 1998). The strongest and most consistent enrichment in LREEs is in barite-dolomite carbonatite. The magnetite-dolomite carbonatite, however, is LREE depleted relative to the other units at Elk Creek and exhibits a significant relative MREE enrichment and minor HREE enrichment. Also notable for the magnetite-dolomite carbonatite is a very strong and consistent enrichment in barium relative to all other units in the carbonatite (Table A1).

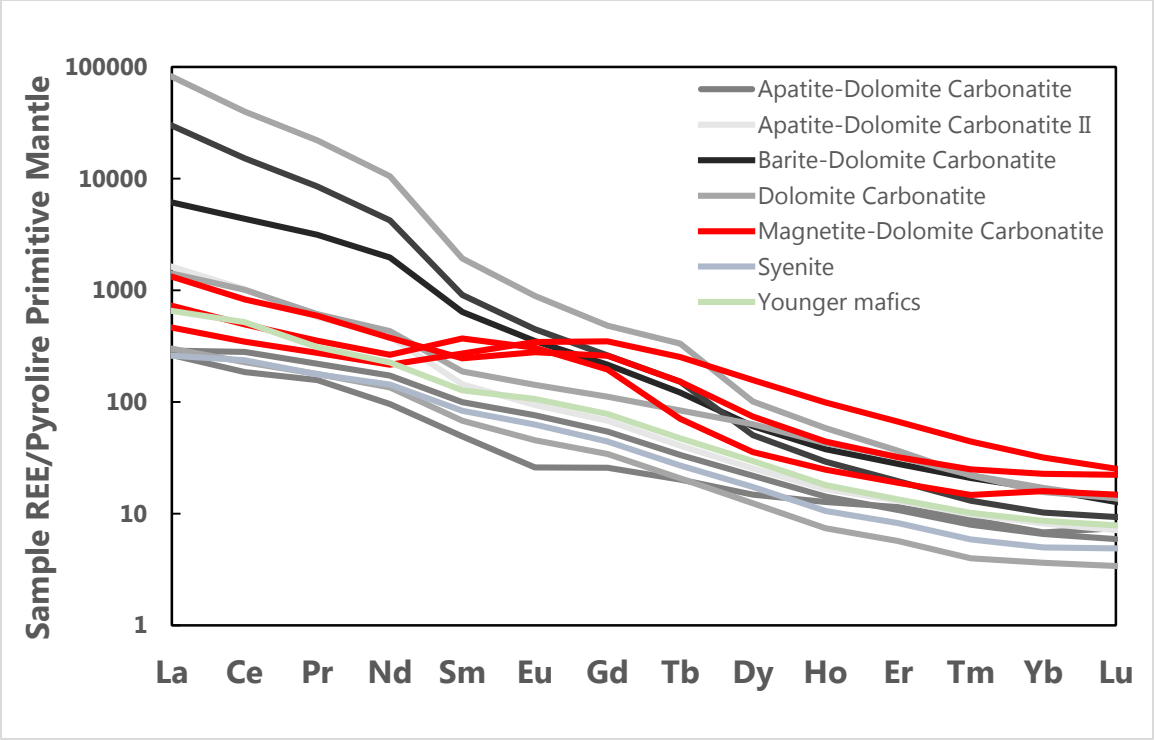

Fig. 25: REE distribution for various lithological units in the Elk Creek Carbonatite Complex, normalized to the pyrolite primitive mantle of McDonough and Sun (1995). The magnetite-dolomite carbonatite anomaly can be seen clearly.

6. Chemical Differences between Pyrochlore Types

6.1 Background

Chemistry provides an additional tool to differentiate between pyrochlore types in the ECCC: Pyrochlore is a niobium mineral, but also an isometric oxide mineral structure with the formula $A_{2-m}B_2X_{6-w}Y_{1-n}$ (Atencio et al., 2010). The pyrochlore mineral structure is flexible and is capable of accommodating a wide range of substitutions (Atencio et al., 2010). The A site is typically occupied by large cations; the B site occupied by HFSEs, and the X and Y sites occupied by anions (less commonly a +1 cation or vacancy) (Atencio et al., 2010). Traditional "stoichiometric" pyrochlore of Hogarth (1977) is of the form $(Ca,Na)_2Nb_2O_6(OH,F)$ but this has been further subdivided by Atencio et al. (2010) depending on Ca/Na and OH/F ratios. Lumpkin and Ewing (1995) indicates that the A and Y sites are susceptible to significant substitution during host-rock alteration; B-site cations, however, are relatively immobile and are a useful tool for differentiating pyrochlore types.

6.2 Results of Microprobe Measurements

The three types of niobium pyrochlore at Elk Creek are relatively similar in their geochemistry, and all plot within the pyrochlore field of the pyrochlore-betafite-microlite solid solution series (Fig. 26A-B). Variations exist, however, that are significant enough to act as a tool for differentiating species of pyrochlore mineralization in the carbonatite complex. Type 1 pyrochlores are zoned concentrically when viewed by backscattered electron imaging, where the brightness (corresponding to higher average atomic number)

is controlled by tantalum enrichment (Fig. 18). Bright bands contain 5-9% Ta_2O_5 while dark bands contain >0.5% Ta_2O_5 and are conversely niobium-enriched. Type 2 pyrochlores are nearly pure niobium pyrochlore, closely approximating stoichiometric composition (Table 2).

Molycorp workers classified ~100 μm euhedral pyrochlore as "generation 2" and ~10 μm euhedral pyrochlore as "generation 3" (Mariano, 1978); the microprobe measurements from this study did not show any significant chemical difference between the two. As a consequence, the two Molycorp classifications have been consolidated into a single "Type 2" pyrochlore. Type 1 pyrochlores have similar chemistry in dark oscillatory zones and in the dark rims; both are different enough from types 2 and 3 (higher F, Ti, lower Na) to support differentiation (Table 2).

Type 3 pyrochlores are slightly depleted in niobium compared to Type 2, without a conjugate enrichment in tantalum (Table 2). Rather, Ti^{4+} appears to be substituting for niobium in the HFSE site. Atencio et al. (2010) identified Ti^{4+} as a substituent for niobium in pyrochlore. The similar charges and atomic radii of six-fold coordinated niobium and tantalum would support this substitution based on Goldschmidt's rules (Faure, 1998).

There is some variation in the cations occupying the A site of the pyrochlore mineral structure. For all types of pyrochlore at Elk Creek, calcium occurs the A site at a higher concentration than sodium. However, Type 2 grains contain sodium at a higher concentration (6-8% vs. 3-4%) compared to Type 1 and Type 3 pyrochlores (Table 2). Uranium substitution is low in all types, with only a few Type 3 grains exceeding 2%

UO_2 (Table 2). Progressive variation is present in the Y anion site; fluorine concentration decreases from Type 1 to Type 3 (Fig. 27) with a calculated conjugate increase in OH concentration. Type 3 pyrochlores contain Sr at higher concentrations relative to the other two types (Table 2). Significant Ba or K was not measured in any of the grains probed.

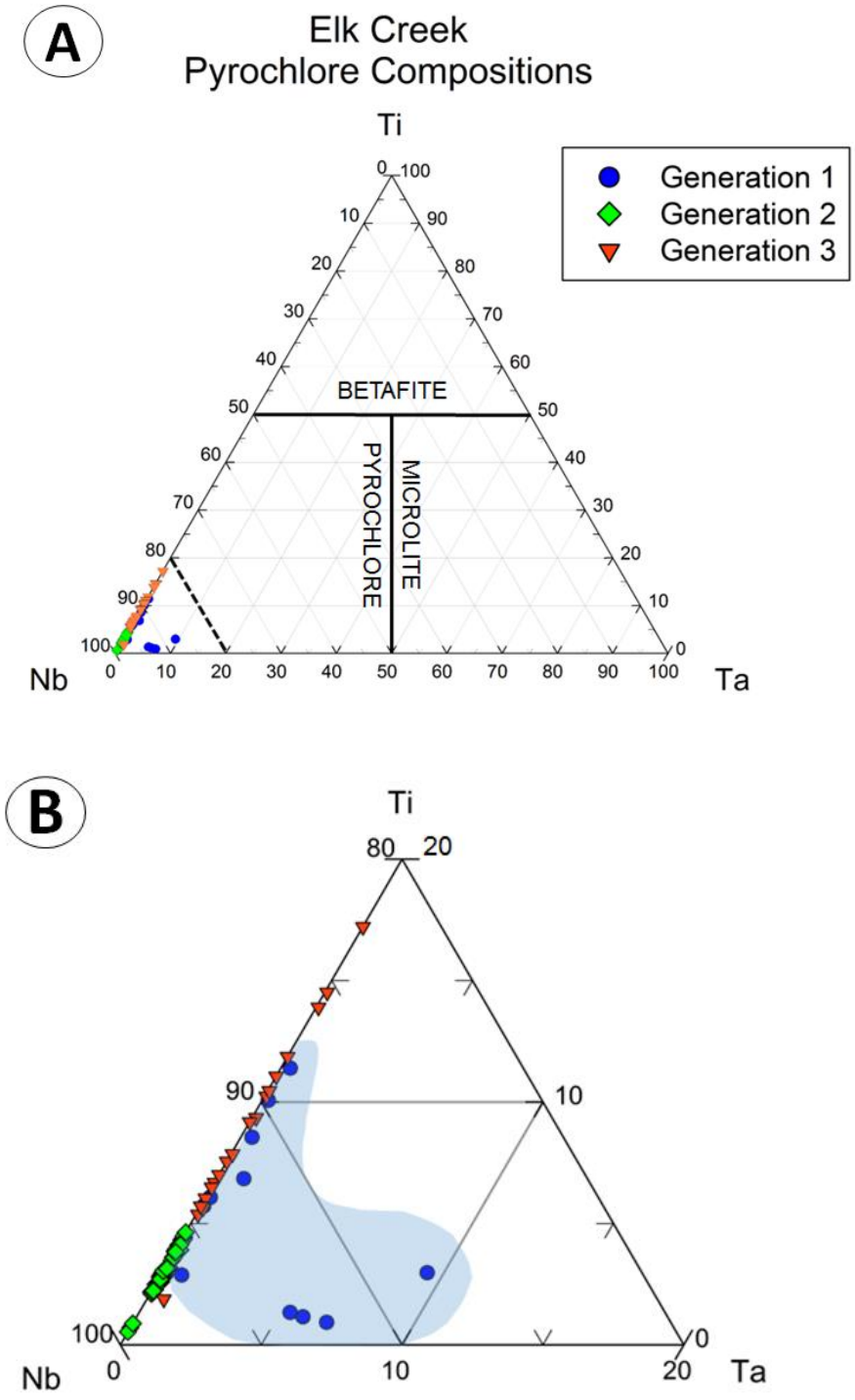

Fig. 26: (A) Ternary diagram of pyrochlore compositions at Elk Creek plotted by B-site high-valence elements. (B) Area enclosed by the dashed line in Fig. 26A.

Table 2: Pyrochlore composition as measured by electron microprobe

	Type 1 **Tantalum-poor**		**Type 1** **Tantalum-rich**		**Type 2**		**Type 3**	
N=	**8**		**5**		**49**		**19**	
	Wt %	**±2σ**	**Wt %**	**±2σ**	**Wt %**	**±2σ**	**Wt %**	**±2σ**
Nb_2O_5	63.3	2.99	56.51	3.61	67.84	5.18	62.28	5.06
Ta_2O_5	0.7	0.74	9.63	5.64	0.1	0.08	0.16	0.41
SiO_2	0.85	1.96	0.34	0.32	0.1	0.3	0.53	0.97
TiO_2	3.01	1.18	0.9	0.72	2.16	1.33	3.67	3.33
ZrO_2	--		--		0.58	1.02	0.38	1.39
ThO_2	0.12	0.23	1.72	1.11	0.22	0.47	1.12	1.5
UO_2	0.12	0.27	1.14	0.88	--[1]		0.43	0.71
Al_2O_3	--		--		1	4.29	0.14	0.27
Y_2O_3	0.01	0.02	0.07	0.05	--[1]		--[1]	
La_2O_3	0.01	0.02	0.01	0.02	0.18	0.09	0.2	0.13
Ce_2O_3	0.22	0.14	0.31	0.08	0.35	0.2	0.55	0.42
Nd_2O_3	0.07	0.05	0.1	0.03	0.11	0.07	0.21	0.11
Fe_2O_3	0.38	0.34	1.11	0.53	0.79	2.49	1.99	2.95
MgO	0.04	0.07	0.01	0.01	0.35	1.58	1.02	2.2
MnO	0.01	0.01	0.01	0.03	0.08	0.14	0.06	0.05
SrO	1.6	1.18	2.38	0.87	1.49	1.74	3.07	2.97
BaO	--		--		0.47	0.83	1.23	2.4
PbO	0.03	0.05	0.21	0.13	0.4	0.11	0.67	0.63
CaO	17.03	1.09	14.52	1.53	15.82	2.11	13.86	3.57
Na_2O	4.6	1.95	3.88	0.76	6.7	3.17	4.37	1.84
K_2O	--		--		0.11	0.04	0.17	0.32
H_2O	--		--		1.01	0.63	1.4	0.48
F	4.89	1.61	3.72	0.58	3.04	1.33	2.03	0.88
O=F	-2.14[2]		-1.62[2]		-1.28[2]		-0.85[2]	
Total	95.12	1.69	95.12	2.88	99.34	2.47	97.05	2.66

[1]Below detection limit
[2]Determined by calculation

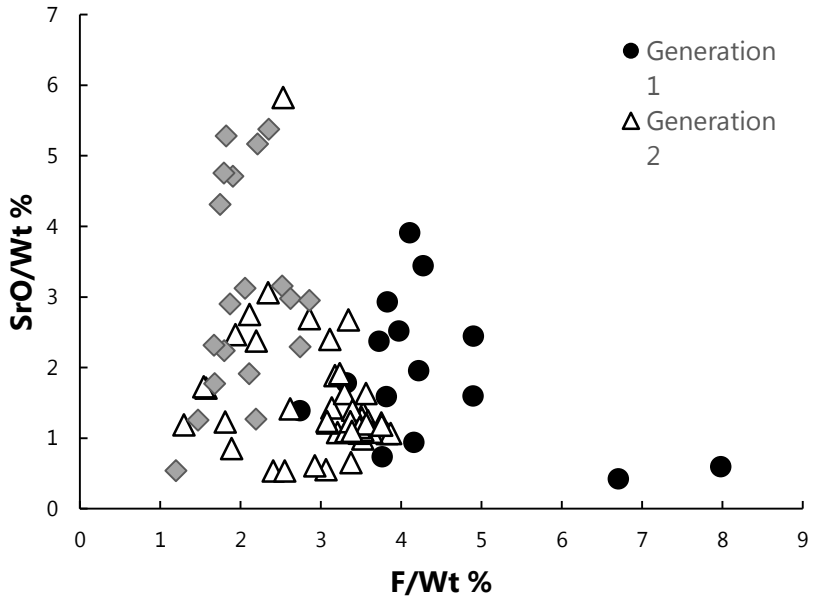

Fig. 27: Binary plot in weight percent for SrO vs F.

REE substitution in all pyrochlores was minor to nonexistent. Type 3 pyrochlores were analyzed for the full suite of rare-earth elements in an attempt to identify the mineral host(s) for the MREE enrichment in magnetite-dolomite carbonatite; no enrichment in MREEs was found in the grains examined. Some Type 3 pyrochlores were slightly enriched in cerium and lanthanum, however (up to 2% Ce+La).

6.3 Microprobe Measurements of Niobian Rutile, Ilmenite, and Magnetite

Grains of magnetite, ilmenite, and rutile in the magnetite-dolomite carbonatite were also analyzed for chemistry with a focus on niobium substitution. Rutile grains were found with detectable concentrations of Nb_2O_5 on the order of 3-10% (Fig. 28). Ilmenite contains minor niobium substitution on the order of 1-3% niobium oxide. Neither rutile nor ilmenite contain detectable concentrations of tantalum. None of the magnetite grains

analyzed contained detectable amounts of niobium or tantalum, and no iron-titanium minerals showed zoning with respect to niobium or tantalum in the magnetite-dolomite carbonatite.

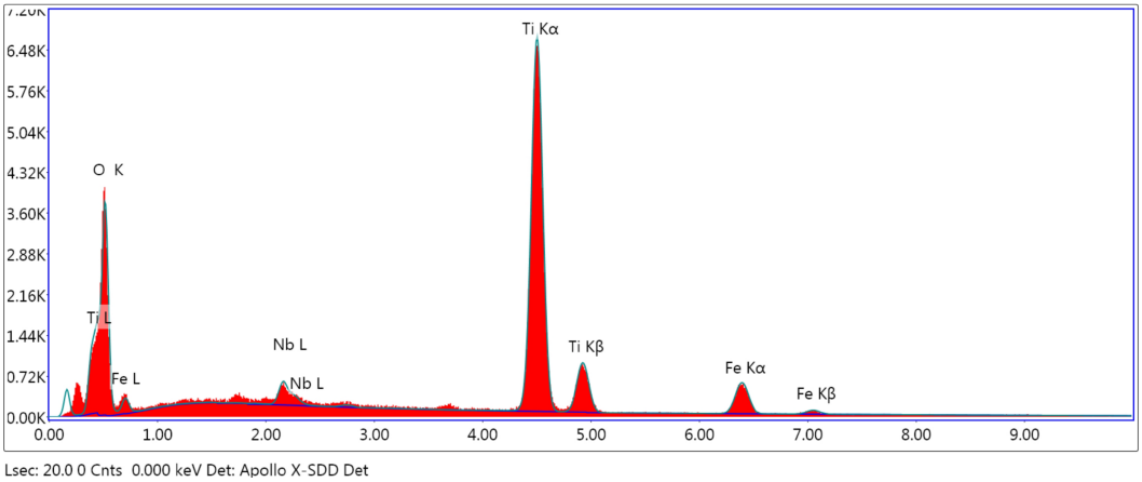

Fig. 28: Energy dispersive spectral analysis showing minor niobium substitution in a rutile grain. Minor iron substitution visible as well (EC-29 1392')

While pyrochlore was the primary target for microprobe geochemistry evaluation, magnetite, ilmenite, and rutile were examined for most major elemental constituents with EDS spectra as a check to detect elements not measured by the microprobe as configured for this work. Magnetite is nearly stoichiometric Fe_3O_4 based on both of these methods but low totals (90-92%) were achieved in microprobe analysis. This may indicate the presence of maghemite which would not visible in backscattered electron imaging; it may also be a consequence of the numerous holes in the magnetite grains, which would significantly increase the difficulty of locating a flat surface for microprobe analysis. Ilmenite in the magnetite-dolomite carbonatite typically has Ti/Fe ratios of 1-1.3:1 with no other major substitutions detected. One grain was found to have MnO on the order of

5% but all others had negligible manganese substitution. Rutile contained consistent minor iron substitution with 3-6% FeO (Fig. 28) but no other detectable chemical components aside from niobium.

7. Discussion

7.1 Assessing the Magnetite-Dolomite Carbonatite

The magnetite-dolomite carbonatite rock in the Elk Creek carbonatite complex is a rare lithology with only a few approximate analogues found in published literature on carbonatite-associated rocks. On a superficial level, the rock bears a resemblance to several carbonatite and felsic peralkaline systems, but none fit well. This may simply be the result of a paucity of discovered analogue systems – carbonatites are relatively rare, and carbonatite-associated rocks with magnetite as a major rock-forming mineral rarer still (Krasnova et al., 2004). There are also complications resulting from the clear later-stage barite-hematite overprinting of the magnetite-dolomite carbonatite, which may have destroyed original mineralogy. There is, however, a possibility that the niobium-bearing magnetite carbonatite at Elk Creek is unique, and only a petrological "first-cousin" to similar systems rather than a true overlapping lithology.

7.1.1 HFSEs: Comparison to Other Carbonatites: Niobium concentrations in the magnetite-dolomite carbonatite are significantly higher than the worldwide averages for all varieties of carbonatite (Table 1). Grades of 0.85 to 1.49% Nb_2O_5 compare favorably to worldwide niobium resources compiled by Mitchell (2014). For other HFSEs, tantalum is present in whole-rock analysis of magnetite-dolomite carbonatite at concentrations

comparable to unmineralized carbonatites – slightly above the average for magnesiocarbonatites, but below the average for phoscorites (Table 1).

The average concentration of Ti in the magnetite-dolomite carbonatite is two-thirds higher than the average for phoscorites and at least 10 times higher than the average carbonatite composition (Table 1). The magnetite-dolomite carbonatite is depleted with respect to Zr when compared to carbonatites worldwide; Hf is at typical concentrations (Table 1). Chakhmouradian (2006) proposes that Nb/Ta and Zr/Hf ratios are more useful than absolute concentrations in understanding the chemical evolution of a carbonatite melt, given the high variability in concentrations seen in compiled values; for both ratios, the magnetite-dolomite carbonatite is atypical (Table 1).

Overall, the pyrolite-normalized HFSE budget for the Elk Creek Carbonatite is unusual in comparison to averages for magnesiocarbonatites/dolomite carbonatites (Fig. 29). The silicate rocks in the ECCC accord reasonably well with typical values for carbonatites compiled by Chakhmouradian (2006) (Table 1), but the Elk Creek dolomite carbonatites are unusually depleted in Zr (Fig. 29). Tantalum concentrations show significant spread, with the barite-dolomite carbonatite depleted relative to all other carbonatite units in the ECCC as well as worldwide carbonatite averages (Table 1). The skewed “v-like” HFSE distribution pattern for the magnetite-dolomite carbonatite is anomalous (Fig. 29). It is not clear what effect alteration might have had on HFSE remobilization, but these data suggest a very unusual fractionation process for generating the magnetite-dolomite carbonatite relative to other carbonatites worldwide or even other rocks in the Elk Creek Carbonatite Complex.

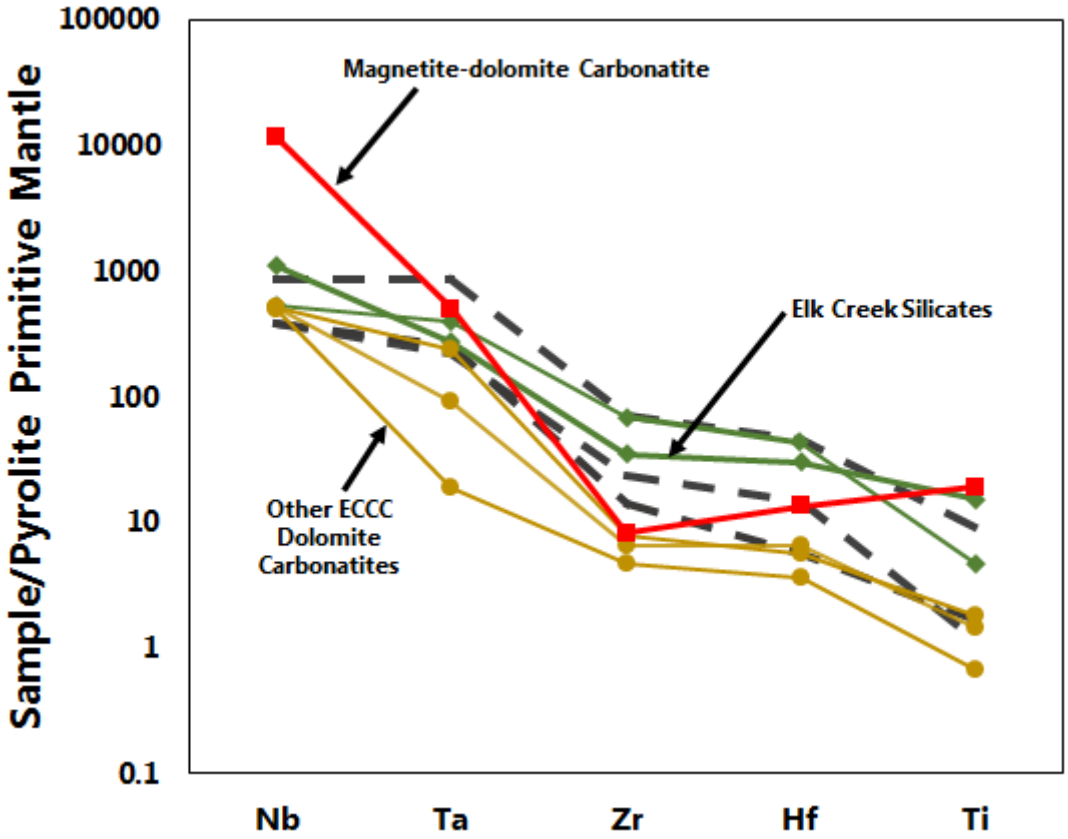

Fig. 29: HFSE distribution pattern for Elk Creek Carbonatite rocks. All values normalized to the pyrolitic primitive mantle of McDonough and Sun (1995). Thick dashed lines represent averages for phoscorites, magnesiocarbonatites, and ferrocarbonatites (top to bottom) compiled by Chakhmouradian (2006).

7.1.2: Potential Genetic Implications from Analogous Rocks: A discussion of the origin of the magnetite-dolomite carbonatite would be aided by a comparison to similar carbonatite-associated rocks with better-understood genetic models. Unfortunately, an exact match has not been reported, and the closest analogues have conflicting genetic models. However, textural evidence from the magnetite-dolomite carbonatite in the ECCC may be useful for future consideration of these rocks.

Phoscorites are rare rocks associated with carbonatites and only a few examples of this rock are known worldwide. The IUGS does not currently have a definition for phoscorites, but the accepted definition is that phoscorite is an igneous rock with the principle rock-forming minerals being magnetite, apatite, and a silicate (forsterite olivine according to Yegorov (1993) and/or phlogopite) (Krasnova et al., 2004). They occur either in direct contact with carbonatite or alkali silicate systems, or are found in the immediate vicinity (Krasnova et al., 2004). These rocks are ultimately derived from the mantle and are believed to be co-magmatic with associated carbonatite rocks (Krasnova et al., 2004). The more immediate petrogenesis of phoscorites, whereby a magnetite-apatite-silicate fluid would separate from a parental carbonatite melt, is less well understood. Some workers propose that phoscorites represent a cumulate formed by density gradients in a carbonatite magma chamber (Lee et al., 2006). Others propose that phoscorites represent an immiscible fluid phase that will separate from a carbonated melt at depth (Lapin, 1982). Experimental petrology by Klemme (2010) did not find evidence of liquid immiscibility in a CaO-MgO-Fe_2O_3-P_2O_5-SiO_2-H_2O-CO_2 system, but noted that fractional crystallization had a very strong effect on the composition of the remaining liquid.

Nelsonites are somewhat similar, with magnetite and apatite as rock-forming minerals without olivine (Kolker, 1982). Titanium is a significant constituent of nelsonites by mass with ilmenite as the principal titanium-bearing mineral. Nelsonites are most typically associated with anorthosites and diorites, but are also associated with carbonatites and alkaline systems such as the Catalao carbonatite complex in Brazil

(Cordeiro et al., 2010). A relatively consistent 2:1 ratio of magnetite+ilmenite/apatite was reported by Kolker (1982) as a common feature of known nelsonite deposits.

The magnetite-dolomite carbonatite in the Elk Creek system bears at least a superficial resemblance to both of these rocks, but there are numerous incongruencies in texture, chemistry, and mineralogy. The magnetite-dolomite carbonatite rock at Elk Creek satisfies the magnetite and apatite requirements, but the silicate minerals (biotite, quartz) are more felsic than a "true" phoscorite. Forsterite is absent and phlogopite is at best a very minor silicate phase observed in dolomite clasts. Neither alteration products of olivine nor pseudomorphs were seen in core evaluated for this work. The mineralogy of the Elk Creek magnetite-dolomite carbonatite does not resemble the results of experimental petrology, but only limited work has been done on these systems (Klemme, 2010). Additionally, apatite is a minor mineral rather than a major rock-forming mineral in the magnetic Elk Creek rocks, and the ratio of magnetite+ilmenite/apatite is much higher than the typical 2:1 ratio observed in nelsonites. Assigning a genetic model proposed for one of these rocks to the magnetite-dolomite carbonatite by way of analogy would be problematic; textural evidence, however, might favor one model over others.

7.1.4 Possible Magmatic Origins: Several lines of evidence exist that suggest that the magnetite-dolomite carbonatite is the result of a discreet pulse of reduced iron-enriched fluid which was emplaced into the carbonatite complex. The brecciated texture seen in many intercepts is evocative of a relatively rapid mode of emplacement such as a vertical-to-subvertical dike swarm which disrupted or entrained wall rock through mechanical fracturing (Sillitoe, 1985). Banding and shearing is at high angles relative to

core axis, as are the elongated porphyroclasts. The Elk Creek Carbonatite is not structurally pristine, but regional tectonic evidence supports straightforward uplift rather than high-angle folding or overturn (Carlson and Treves, 2005).

The pyrochlore associated with the magnetite-dolomite carbonatite is geochemically distinct from pyrochlore hosted in other carbonatite lithologies, based on alteration-resistant B-site cation substitution. It is, however, somewhat similar to Type 2 pyrochlores (Figure XYZ) and none of the types are substantially different in comparison to other pyrochlore deposits worldwide: As a point of comparison, pyrochlore crystals in the Sokli carbonatite-phoscorite complex identified as primary contain 11-13% Ta_2O_5 and 11-22% UO_2 (Lee et al., 2006). The magnetite-dolomite carbonatite also has a characteristic and unusual REE distribution pattern, although the nature of the MREE enrichment is still under investigation.

The more proximal origin of the melt is less clear, however. Experiments by Klemme (2010) did not find evidence of an immiscibility gap with respect to phoscorite-like melts. However, small variations in P concentration can have significant consequences for the overall behavior of a melt, and the typical P_2O_5 concentrations of the magnetite-dolomite carbonatite at Elk Creek are lower than the 1.1% that formed the low end of experiments by Klemme (2010). The origin of a magnetite-dolomite carbonatite through fluid immiscibility from a parent dolomitic melt is conceivable based on general experimental work on conjugate silicate-carbonate fluids (Kjarsgaard and Hamilton, 1988) but field evidence in the ECCC is lacking. The dolomite clasts in magnetite-dolomite carbonatite have relatively sharp contacts with the matrix but do not

resemble the spherical, laterally-continuous immiscibility ocelli reported in Kjarsgaard and Hamilton (1988). What is clear is that the magnetite-dolomite carbonatite underwent an unusual degree of magmatic fractionation relative to the other carbonatite rocks at Elk Creek, as well as in comparison to "average" carbonatites and phoscorites (Table 1). Small variations in HFSEs could conceivably reflect heterogeneity in the upper mantle, but the highly unusual HFSE pattern seen in the magnetite-dolomite carbonatite is puzzling.

The formation of cumulates may still be an important or even primary contributor to the immediate petrogenesis of the magnetite-dolomite carbonatite. Downes et al. (2005) propose accumulation as the primary petrogenetic model for many of the carbonatites in the Kola Alkaline Province based on gradational mineralogy and geochemistry. The magnetite-dolomite carbonatite does not contain exotic minerals which are absent from other rocks in the ECCC; only the relative proportions of mineral species by volume is different. Additionally, the very minor alteration haloes surrounding the dolomite clasts suggests that the temperature and chemical difference between the clasts and the matrix was small. The overall size and volume of the Elk Creek complex suggests a large magma chamber with a significant vertical component. Disruption and brecciation of an emplaced dolomite carbonatite at the top of the chamber would generate fragments that would sink into the melt and could settle into a mush of dense minerals and dolomite clasts deeper in the crust. This mush could then be stirred up by subsequent pulses of low-viscosity carbonatite melt and redistributed elsewhere in the intrusive complex.

Some textural evidence in the magnetite-dolomite carbonatite is ambiguous, or in opposition to the cumulate model. The magnetite-dolomite carbonatite is relatively fine-grained, with magnetite and ilmenite grains rarely exceeding 200 μm in longest dimension. The magnetite-dolomite carbonatite also contains significant banding and shearing of dolomite-carbonatite fragments (but not individual mineral grains). Some mm-sized bands are more densely-packed with magnetite, resembling a cumulate texture, but the rock as a whole does not show regular changes in density or mineralogy down-hole or across intercepts. This is in contrast to traditionally-understood cumulate systems such as the Stillwater complex of Montana, which features cumulate textures and changes in mineralogy evocative of mineral sorting by density (Todd et al., 1982). However, the extremely low viscosity of carbonatites may not allow for the placid settling of crystals in a magma chamber – turbulent and disruptive flow would wipe away such features (Treiman and Scheidl, 1983).

Based on Seifert et al. (2000) the magnetite-dolomite carbonatite shares some textural similarities to a dolomite (beforsite) breccia occurring in a diatreme that intruded explosively into the Delitzsch ultramafic-carbonatite complex. This breccia contains rounded fragments of older dolomite, xenocrysts, and angular wall rock fragments in a matrix of ferroan dolomite with accessory pyrochlore (Seifert et al., 2000). An explosive eruption of a carbonatite fluid as proposed by Seifert et al. (2000) could both shatter carbonatitic wall rock as well as entrain heavy minerals accumulating at the bottom of an existing partially-molten magma chamber. The depletion in F in the Type 3 pyrochlores may be an additional line of evidence for a more extrusive/explosive style for the

magnetite-dolomite carbonatite if trends identified by Bambi et al. (2012) hold true. However, no wall-rock xenoliths have been observed in the magnetite-dolomite carbonatite thus far; the violent and explosive ascent of a diatreme would be expected to entrain older wall rocks as well. The geometry for the magnetite-dolomite carbonatite interpreted by Drenth (2014) indicates a slight widening at depth which contradicts the opening-upwards funnel shape of a diatreme. Low F in pyrochlore may also be indicative of alteration rather than a reflection of original melt composition (Lumpkin and Ewing, 1995).

The petrogenesis of the magnetite-dolomite carbonatite presents a vexing problem: Calling it either a breccia-like cumulate or a breccia with cumulate-like features would be defensible by different lines of evidence, and barite overprinting and iron oxidation are pervasive features which may obscure critical aspects of the original rock. Textural evidence suggests a pulse of iron-rich carbonatite fluid which brecciated and fragmented a previously-emplaced carbonatite rock, but accumulation may have been involved in this process as well.

7.2 Styles of Alteration in the ECCC

The widespread and diverse alteration styles observed in the Elk Creek Carbonatite suggest that post-magmatic fluids were a critical component of the complex's formation. Alteration is not the primary focus of this paper, but a few preliminary conclusions can be drawn from observations: The initial magnetite-dolomite carbonatite melt was relatively reduced, precipitating ferrous minerals such as ilmenite and magnetite, and partially flooding dolomite clasts with ferrous iron (Fig. 8B). These rocks were pervasively

overprinted by significantly more oxidizing and sulfur-rich fluids which disrupted and replaced original rock, ending with the widespread emplacement of barite, apatite, secondary dolomite, and pyrite. Veins containing these minerals were also emplaced at this stage, cutting across all major lithologies in the ECCC.

The cloudy appearance and irregular boundaries of euhedral dolomite grains in contact with apatite and barite (Figs. 5, 15) supports the interpretation that apatite and barite are secondary. These fluids were also enriched in SiO_2, precipitating quartz. The emplacement of REE-bearing minerals is a feature of this later stage, potentially controlled by local chemical conditions; barite veinlets are not REE-enriched in the magnetite-dolomite carbonatite, but zones of pervasive barite and/or apatite mineralization in dolomite carbonatite elsewhere in the complex can be strongly REE-enriched.

There was also some aspect of the magnetite-dolomite carbonatite which made it especially susceptible to alteration; secondary barite is a pervasive feature in the unit, occurring as disseminations, mineral overgrowths, veins, and patches. BaO concentrations in samples of magnetite-dolomite carbonatite are in the range of 6-10%, a substantial contribution to whole-rock geochemistry (Table A1). Speculation about the original mineral assemblage of the magnetite-dolomite carbonatite is difficult, but substantial overprinting indicates that the modal mineralogy and mineral phases observed today may be vastly different than what was originally emplaced by the iron-enriched carbonatite melt.

Alteration also adds an additional challenge to tracing the origin of the magnetite-dolomite carbonatite melt via high field strength elements; while HFSEs are considered relatively immobile under a wide range of conditions, the presence of high concentrations of sulfate, fluorine, and phosphate ions can mobilize these elements through acting as complexing agents (Jiang, 2005). The ability of these factors to control the distribution of HFSEs is less clear, however, and the distribution of these elements in the magnetite-dolomite carbonatite (Fig. 29) is unlike that of barite or apatite-altered dolomite carbonatite. The mineral hosts of Nb, Ta, and Ti also appear to precede alteration, suggesting that the original magmatic fluid was still unusual with respect to HFSE fractionation.

7.3 Niobium Mineralization and Pyrochlore Paragenesis

7.3.1. Comparison to other Niobium Deposits: Pyrochlore at Elk Creek is morphologically distinct compared to other major primary niobium deposits in the world. The nelsonite-hosted pyrochlore in the Catalao complex is 100 μm or larger in longest dimension, and is yellow-orange or brown-green in thin-section (Cordeiro et al., 2011). Pyrochlores from the Sokli carbonatite are reported as typically larger than 2 mm diameter with only very rare euhedral grains smaller than 100 μm (Lee et al., 2006). Oka pyrochlores are poikolitic overgrowths on latrappite with a diameter up to 3 mm (Chakhmouradian, 1996). Type 1 pyrochlore grains in the ECCC are somewhat similar to other examples in literature, but Type 3 grains are atypical. This is especially notable due to their large contribution to the overall niobium resource at Elk Creek. Cordeiro et al. (2011) references pyrochlore inclusions in ilmenite in the Catalao Carbonatite Complex,

but the morphology of those pyrochlores is not indicated and the chemistry is not specified. References to niobian rutile in literature are scant; references to pyrochlore inclusions in dolomite or magnetite are almost nonexistent and no direct analogues to Type 3 pyrochlore are found in literature review.

7.3.2 Potential Sources and Chemical Constraints on Niobium in the ECCC: Pyrochlore has been identified as a mineral which will crystallize out of a primary magmatic melt relatively early in the emplacement of an igneous body such as a carbonatite (Mitchell, 2014). Mantle-derived carbonatites are believed to be products of low degrees of partial melting of carbonated peridotite and lherzolite – A fluid derived from this partial melting would be significantly enriched in incompatible elements including niobium and other HFSEs (Chakhmouradian, 2006). Additional fractionation is needed to form an ore-grade niobium deposit, however, and several possible mechanisms have been proposed including fractional crystallization, and accumulation followed by disaggregation and rheology-controlled redistribution (Mitchell, 2014).

The absence of other niobium-bearing mineral phases in the ECCC constrains the chemistry of the initial niobium-enriched melt. In other carbonatite-alkaline systems worldwide, a perovskite-group mineral named lueshite ($NaNbO_3$) is the primary host of niobium, forming under different chemical conditions. The Lesnaya Varaka complex on the Kola Peninsula of northern Russia is an example of this: A multi-stage apatite-dolomite carbonatite-alkaline system containing primary lueshite and niobium loparite ($Na_{1/2}REE_{1/2}TiO_3$) as niobium mineral phases with pyrochlore as an overgrowth/secondary rim on lueshite (Chakhmouradian & Mitchell, 1998). A key

difference between this complex and the ECCC, however, is the presence of early primary fluoroapatite and a relatively high initial concentration of Na in the melt. Perovskite-group minerals require both a high activity of Na to form, as well as an absence of F, P, and OH to complex with niobium ions (Chakhmouradian & Mitchell, 1998). The absence of perovskite in the ECCC suggests that Na activities in the melts were low, and complexing agents were available.

Curiously, whole-rock concentrations of fluorine in magnetite-dolomite carbonatite are below the concentration necessary to form pyrochlore. Experimental observations by Mitchell and Kjarsgaard (2004) identify F and P as critical complexing elements which transport Nb and result in precipitation of pyrochlore. Bambi et al. (2012) proposes that a minimum melt concentration of 1% F is required for pyrochlore formation, a concentration significantly higher than the 0.1-0.2% seen in the magnetite-dolomite carbonatite at Elk Creek (Table A1). Another niobium-bearing mineral phase would be expected to occur in the magnetite-dolomite carbonatite instead, such as lueshite (Mitchell and Kjarsgaard, 2004). Concentrations of F and P in mineralized dolomite carbonatite in the ECCC are higher and may be expected to allow pyrochlore crystallization, though F is still slightly below the critical 1% threshold (Table A1). It is not clear why the whole-rock geochemistry does not support pyrochlore crystallization in the magnetite-dolomite carbonatite, but fluorine is a secondary alteration mineral throughout the complex and may have remained in the residual fluid after the emplacement of the magnetite-dolomite carbonatite rock.

The crystal chemistry of pyrochlore is susceptible to miniscule changes in the chemistry of a melt, and has a flexible structure capable of accommodating a considerably vast number of substitutions. Other workers have identified a potential framework paragenetic sequence for pyrochlore using elemental substitution in the pyrochlore mineral structure as a marker. The earliest and most "primitive" pyrochlores have significant tantalum substitution based on field studies of other carbonatite-hosted pyrochlore deposits (Mitchell, 2014). Stoichiometric (Ca,Na, Nb) pyrochlore is identified as the product of a more evolved magmatic fluid (Hogarth et al., 2000).

Type 1 and 2 pyrochlores are typically found as euhedral inclusions in dolomite, apatite, and rarely barite. If the paragenetic sequence for pyrochlore in other carbonatite complexes is robust, then Type 1 pyrochlores may have been the first to crystallize in the ascending carbonatite magma column which fed the ECCC. The presence of fragments of Type 1 pyrochlore in the relatively early magnetite-dolomite carbonatite supports the notion that precipitation of this type of pyrochlore occurred very early in the formation of the complex; however, the presence of Type 1 pyrochlores in later biotite-bearing dolomite carbonatite confounds this generalization. Type 2 and 3 pyrochlores crystallized in a comparatively Ta-poor fluid, though assigning a genetic order to Type 2 pyrochlores based on chemistry would be contradicted by field evidence; Type 2 pyrochlores occur in both early and late dolomite carbonatite. The wide range of carbonatite lithologies and cross-cutting relationships at Elk Creek suggest multiple pulses of carbonatite magma entering the system over a period of time.

Regarding the problem of how Type 1 and 2 pyrochlores can be set in both early and late carbonatite rocks, the relatively small intervals of ore-grade niobium enrichment in dolomite carbonatite might represent a gravity fractionation of heavy minerals in a circulating melt brought up from a deeper magma chamber. Carbonatite melts are ionic fluids with very low viscosity, capable of turbulent flow and rapid convection currents (Treiman and Schedl, 1983). With a specific gravity of ~5 g/cm^3, a 1 mm pyrochlore crystal would very rapidly sink in a dolomite carbonatite melt. Subsequent pulses of magma could disaggregate reservoirs of crystallized pyrochlore deep in the magma chamber, redistributing it throughout the carbonatite complex (Mitchell, 2014).

However, Type 1 pyrochlore would have had to remain in place for some time during cooling in order to develop oscillatory zonation; Hogarth et al. (2000) propose a disequilibrium-feedback mechanism for oscillatory-zoned pyrochlore. In this model, small changes in chemistry in the fluid and small differences in Nb and Ta solubility would lead to cycles of supersaturation of one element, precipitation, then undersaturation and build-up of that one element at the crystal-fluid interface while the other element is preferentially incorporated (Hogarth et al., 2000).

7.3.3 A Paragenetic Sequence for Type 3 Pyrochlore: Relations with surrounding minerals can shed some light on the paragenetic sequence of Type 3 pyrochlore at Elk Creek. A few grains are seen in contact with magnetite, but grains in equilibrium contact with ilmenite are more common. Rutile is in contact with pyrochlore but pyrochlore inclusions in rutile crystals are rare. Barite is not typically seen in direct contact with pyrochlore and Type 3 pyrochlores have only very minor barium substitution. Pyrochlore

is occasionally seen as inclusions in barite but this is a localized phenomenon and may be related to destruction of less-resistant minerals that were hosting pyrochlore inclusions.

The most likely scenario for the niobium mineralization in magnetite-dolomite carbonatite (Fig. 30) is that pyrochlore crystallization peaked during ilmenite crystallization and concluded during magnetite crystallization. Before this point, niobium entered into rutile as a minor substitute. Rutile appears in the cores of rutile-ilmenite aggregates (Fig. 24), has a pitted, partially-skeletal appearance elsewhere (Fig. 23), and appears to be an early mineral in the magnetite-dolomite carbonatite. Ilmenite either agglomerated onto these rutile grains, or may represent an overgrowth or alteration rim. Inclusions of euhedral pyrochlore in magnetite indicate crystallization before magnetite, but anhedral inclusions and embayments are more difficult to constrain and may indicate co-crystallization. The bulk of Type 3 pyrochlore mineralization took place during the crystallization of ilmenite, as indicated by the relative abundance of pyrochlore inclusions in ilmenite aggregates compared to magnetite or rutile, and the lack of euhedral pyrochlore in ilmenite relative to magnetite. The free-floating subhedral-euhedral grains in dolomite are more difficult to constrain, but given their similar geochemistry it would seem reasonable to conclude that they crystallized during similar melt conditions. Magnetite may have incorporated these free-floating grains as inclusions. It is not clear whether pyrochlore crystallization occurred *in situ* in an emplaced, cooling crystal mush or at deeper levels of the magma chamber in a fluid melt. The latter explanation seems more plausible given the apparent original euhedral shapes of the magnetite and ilmenite which host pyrochlore inclusions.

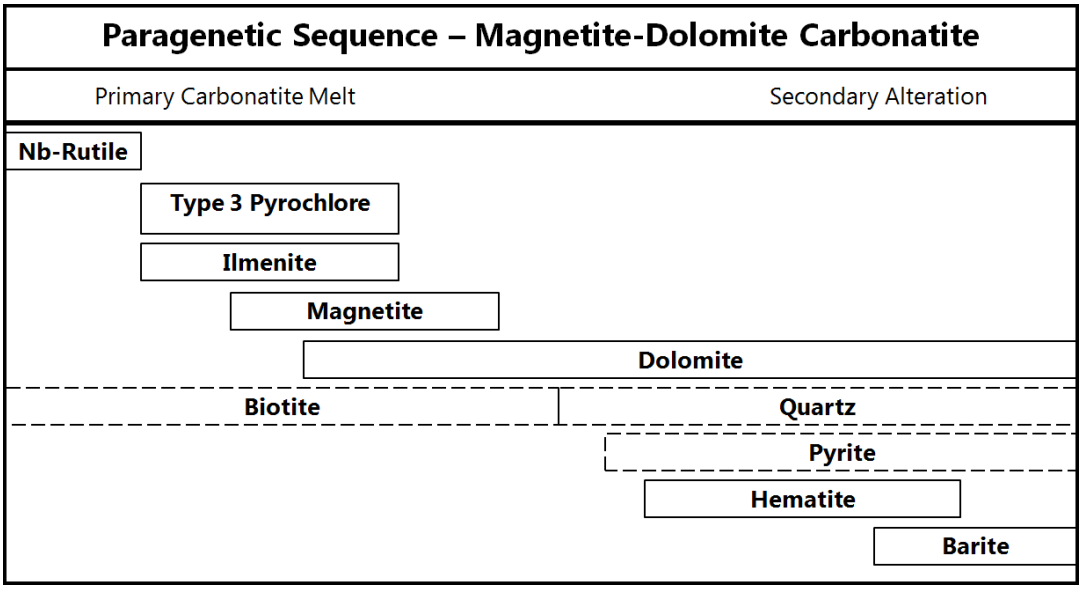

Fig. 30: Proposed paragenetic sequence for niobium mineralization in the magnetite-dolomite carbonatite.

Assigning a temporal or evolutionary trend to all of the pyrochlore types across all of the lithological units at Elk Creek may not be possible using chemistry or geological field evidence. Researchers have identified that tantalum substitution tends to be a signifier of early pyrochlore, but trends outside of this tend to be more ambiguous (Mitchell, 2014). Titanium substitution in Type 3 pyrochlore is a good identifying characteristic that is not a result of secondary alteration – the B site in the pyrochlore structure is very resistant to remobilization compared to the A site (Lumpkin and Ewing, 1995). This enrichment is likely to be a reflection of the chemistry of the original melt in which the pyrochlore precipitated. Field evidence is also ambiguous for Type 1 and Type 2 pyrochlore; these grains reside in both early and late carbonatite rocks.

7.3.4 Post-Emplacement Alteration of ECCC Pyrochlore: Evidence of later-stage alteration is ambiguous with respect to the pyrochlore types at Elk Creek. Lumpkin and Ewing (1995) identify several geochemical trends associated with the alteration of pyrochlore based on field studies of altered, pyrochlore-bearing pegmatites, syenites, and carbonatite rocks. Initial high-temperature fluid alteration is associated with depletion in Ca, Na, and F and conjugate enrichment in Sr, O, Mn, Ba, and Fe (Lumpkin and Ewing, 1995). Later-stage alteration increases concentrations of REE and Fe (Lumpkin and Ewing, 1995). Substantially increased barite concentration is associated with strong alteration and laterization with a trend towards bariopyrochlore (Ca and Na replaced entirely with Ba) with A-site and Y-site vacancies (Williams et al., 1997). Sr concentration in Type 3 pyrochlores is higher than in the first and second types (Fig. 27), and is similar to the Sr concentration in some altered pyrochlores described by Lumpkin and Ewing (1995). Lumpkin and Ewing (1995) added the qualification, however, that primary carbonatite melts can be enriched in elements like Sr and Fe; in this model, substitution in pyrochlore would reflect the composition of the original carbonatite fluid.

Barium concentrations in all ECCC pyrochlore types are either low or nonexistent, with Type 3 pyrochlores only occasionally exceeding 2% BaO. The relationship between barium and alteration is less straightforward with the exception of late low-temperature and supergene alteration (Torró et al., 2012). Potassium has been identified by other workers as another proxy element for lattice vacancies, another indicator of weathering or alteration (Lumpkin & Ewing, 1995). None of the pyrochlore grains examined from the Elk Creek carbonatite contained measurable potassium.

The relative enrichment in Sr, Ba and Fe in Type 3 pyrochlores may be evidence of relatively uniform and pervasive low-grade alteration which resulted from high temperature fluid-rock interaction. If the enrichment of these elements in Type 3 pyrochlore is not a reflection of the initial melt chemistry, the later hydrothermal fluid which emplaced barite and oxidized magnetite to hematite in the magnetite-dolomite carbonatite would be the most likely driver of Type 3 pyrochlore alteration.

8. Conclusions

The Elk Creek Carbonatite comprises a diverse suite of carbonatite and silicate rocks, each possessing a unique chemistry and petrology. This complexity attests to a history of magmatic fluid injections, hydrothermal overprinting, and mechanical disruption. Mineralization of pyrochlore at Elk Creek is only a small part of the whole system and further discoveries are inevitable with new drilling and (potential) mining. However, based on geochemical and geological analysis conducted on existing boreholes, several statements can be made regarding the origin of the magnetite-dolomite rock in the ECCC, its relationship to the other carbonatite rocks in the complex, and its characteristic niobium enrichment:

1) The Elk Creek Carbonatite Complex comprises a largely-dolomitic carbonatite with a subordinate magnetite-dolomite carbonatite as a separate igneous phase. Subsequent alteration of the dolomite carbonatite by increasingly oxidizing and sulfur-rich fluids produced most of the apparent variety of carbonatite rocks in the complex (apatite-dolomite carbonatite, barite-dolomite carbonatite, etc.)

2) The magnetite-dolomite carbonatite which hosts the highest consistent niobium grades is an atypical variant of a family of magnetite-rich rocks associated with carbonatite, alkaline, and anorthositic systems. Geochemistry and mineralogy are somewhat similar to phoscorites and nelsonites, but the magnetite-dolomite carbonatite cannot be easily classified as either. Distribution of HFSE elements in the magnetite-dolomite carbonatite suggests an unusual fractionation process at work relative to other carbonatites. Secondary alteration must be considered as a possible confounding factor to understanding the geochemistry of this unit, as reflected by pyrochlore crystallization contradicting whole-rock geochemistry.

3) Textural evidence suggests that the magnetite-dolomite carbonatite was emplaced in a disruptive event which entrained fragments of dolomite carbonatite into a melt. This event may have disrupted a partially-molten cumulate at the base of the magma chamber and redistributed heavy minerals into a near-vertical flow which formed dikes and plugs in a pre-existing “warm” carbonatite.

4) Niobium pyrochlore is the predominant niobium mineral phase at Elk Creek, with niobian rutile adding the small remaining contribution to the whole. Melt composition during the emplacement of the Elk Creek carbonatite did not vary outside of a fluorine-bearing, relatively alkali-poor fluid.

5) Morphological and geochemical variations are sufficient enough to break the niobium pyrochlore mineralization in the Elk Creek Carbonatite into at least three different species: 1) A tantalum-rich, concentrically zoned first type consisting of relatively large amber-colored pyrochlore; 2) a second type with a straightforward Na-Ca

composition; and 3) a third type of very small, Ti-enriched pyrochlore grains endemic to the magnetite-dolomite carbonatite. Chemical trends are not sufficient to identify a complete paragenetic order for pyrochlore mineralization, and field evidence is ambiguous. Chemical evidence for significant pyrochlore alteration or laterization is not present in the grains probed in the ECCC; slight Sr and Ba substitution in Type 3 pyrochlores may indicate high-temperature fluid alteration but may also reflect the composition of the primary melt.

6) A paragenetic order can be established for pyrochlore in the magnetite-dolomite carbonatite based on relationships between minerals, mineral alteration, and increasingly oxidizing conditions from rutile to barite+hematite. Small amounts of niobium were in rutile as a substitute before pyrochlore crystallization. A significant amount of pyrochlore mineralization occurred during the crystallization of ilmenite, and conjugate element substitution aided the formation of these aggregates. More euhedral pyrochlore grains were incorporated into magnetite largely as inclusions and pyrochlore crystallization was largely complete at this point. Likely complexing elements are F and P for niobium in the melt as per primary experiments, but it is not clear how these elements were removed as the magnetite-dolomite carbonatite lacks these elements in sufficient amounts to allow for pyrochlore crystallization – Niobium perovskite would be expected if current geochemistry reflected melt geochemistry.

The association between magnetite-dolomite carbonatite and niobium mineralization is fairly robust throughout the Elk Creek system, and this association can be used to guide further exploration efforts and mining. Geometry and geophysics

suggest that the plug of magnetite-dolomite carbonatite will extend downwards rather than laterally. It can also be reasonably expected that the style of niobium mineralization will be similar – very small pyrochlore grains included in magnetite and ilmenite, supplemented by small free-floating grains in the matrix and in dolomite carbonatite clasts.

9. References

Atencio, D., Andrade, M.B., Christy, A.G., Gieré, R., and Kartashov, P.M., 2010, The pyrochlore supergroup of minerals: nomenclature: The Canadian Mineralogist, v. 48, p. 673-698.

Bambi, A., Costanzo, A., Gonçalves, A., and Melgarejo, J., 2012, Tracing the chemical evolution of primary pyrochlore from plutonic to volcanic carbonatites: the role of fluorine: Mineralogical Magazine, v. 76, p. 377-392.

Carlson, M., and Treves, S., 2005, The Elk Creek Carbonatite, southeast Nebraska–an overview: Natural Resources Research, v. 14, p. 39-45.

Chakhmouradian, A.R., 2006, High-field-strength elements in carbonatitic rocks: geochemistry, crystal chemistry and significance for constraining the sources of carbonatites: Chemical Geology, v. 235, p. 138-160.

Chakhmouradian, A.R., 1996, On the development of niobium and rare-earth minerals in monticellite-calcite carbonatite of the Oka complex, Québec: The Canadian Mineralogist, v. 34, p. 479-484.

Chakhmouradian, A., and Mitchell, R., 1998, Lueshite, pyrochlore and monazite-(Ce) from apatite-dolomite carbonatite, Lesnaya Varaka complex, Kola Peninsula, Russia: Mineralogical Magazine, v. 62, p. 769-782.

Cordeiro, Pedro Filipe de Oliveira, Brod, J.A., Palmieri, M., de Oliveira, C.G., Barbosa, E.S.R., Santos, R.V., Gaspar, J.C., and Assis, L.C., 2011, The Catalão I niobium deposit, central Brazil: Resources, geology and pyrochlore chemistry: Ore Geology Reviews, v. 41, p. 112-121.

Cordeiro, P.F., Brod, J.A., Dantas, E.L., and Barbosa, E.S., 2010, Mineral chemistry, isotope geochemistry and petrogenesis of niobium-rich rocks from the Catalão I carbonatite-phoscorite complex, Central Brazil: Lithos, v. 118, p. 223-237.

Dicken, C.L., Pimley, S.G., and Cannon, W.F., 2001, Precambrian basement map of the northern midcontinent, U.S.A. -- A digital representation of the 1990 P.K. Sims map: U.S. Geological Survey Open-File Report 01-021, http://pubs.usgs.gov/of/2001/of01-021/

Downes, H., Balaganskaya, E., Beard, A., Liferovich, R., and Demaiffe, D., 2005, Petrogenetic processes in the ultramafic, alkaline and carbonatitic magmatism in the Kola Alkaline Province: a review: Lithos, v. 85, p. 48-75.

Drenth, B.J., 2014, Geophysical expression of a buried niobium and rare earth element deposit: The Elk Creek carbonatite, Nebraska, USA: Interpretation, v. 2, p. SJ169-SJ179.

Farmer, G., Kettler, R., and Verplanck, P., Geochemical and isotropic constraints on the age and origin of the Elk Creek carbonatite complex, SE Nebraska: Geological Society of America Abstracts with Programs, Vol. 45, No. 5, p.41.

Faure, G., 1998, Principles and applications of geochemistry: a comprehensive textbook for geology students: Prentice Hall, 625 p.

Hogarth, D., 1977, Classification and nomenclature of the pyrochlore group: American Mineralogist, v. 62, p. 403-410.

Hogarth, D., Williams, C., and Jones, P., 2000, Primary zoning in pyrochlore group minerals from carbonatites: Mineralogical Magazine, v. 64, p. 683-697.

Horning-Kjarsgaard, I., 1998, Rare earth elements in sövitic carbonatites and their mineral phases: Journal of Petrology, v. 39, p. 2105-2121.

Jiang, S., Wang, R., Xu, X., and Zhao, K., 2005, Mobility of high field strength elements (HFSE) in magmatic-, metamorphic-, and submarine-hydrothermal systems: Physics and Chemistry of the Earth, Parts A/B/C, v. 30, p. 1020-1029.

Kjarsgaard, B., and Hamilton, D., 1988, Liquid immiscibility and the origin of alkali-poor carbonatites: Mineralogical Magazine, v. 52, p. 43-55.

Klemme, S., 2010, Experimental constraints on the evolution of iron and phosphorus-rich melts: experiments in the system CaO-MgO-Fe2O3-P2O5-SiO2-H2O-CO2: Journal of Mineralogical and Petrological Sciences, v. 105, p. 1-8.

Knudsen, C., 1989, Pyrochlore group minerals from the Qaqarssuk carbonatite complex, *in* Lanthanides, Tantalum and Niobium: Springer, p. 80-99.

Kolker, A., 1982, Mineralogy and geochemistry of Fe-Ti oxide and apatite (nelsonite) deposits and evaluation of the liquid immiscibility hypothesis: Economic Geology, v. 77, p. 1146-1158.

Krasnova, N., Petrov, T., Balaganaskaya, E., Garcia, G., Moutte, J., Zaitsev, A., and Wall, F., 2004, Introduction to phoscorites: occurrence, composition, nomenclature and petrogenesis, *in* Wall, F. and Zaitsev, A.N., eds., Phoscorites and Carbonatites from Mantle to Mine: the Key
Example of the Kola Alkaline Province. London, The Mineralogical Society Series, p. 99.

Lapin, A., 1982, Carbonatite differentiation processes: International Geology Review, v. 24, p. 1079-1089.

Le Maitre, R.W., Bateman, P., Dudek, A., Keller, J., Lameyre, J., Le Bas, M., Sabine, P., Schmid, R., Sorensen, H., and Streckeisen, A., 1989, A classification of igneous rocks and glossary of terms: Recommendations of the International Union of Geological Sciences Subcommission on the Systematics of Igneous Rocks: Blackwell Oxford, 193 p.

Lee, M.J., Lee, J.I., Garcia, D., Moutte, J., Williams, C.T., Wall, F., and Kim, Y., 2006, Pyrochlore chemistry from the Sokli phoscorite-carbonatite complex, Finland: Implications for the genesis of phoscorite and carbonatite association: Geochemical Journal-Japan-, v. 40, p. 1.

Lumpkin, G.R., and Ewing, R.C., 1995, Geochemical alteration of pyrochlore group minerals: pyrochlore subgroup: American Mineralogist, v. 80, p. 732-743.

Machel, H., 1985, Cathodoluminescence in calcite and dolomite and its chemical interpretation: Geoscience Canada, v. 12, p. 139-147.

Mariano, A., 1978, A Study of the Petrology and Niobium Mineralization in Drill Core from EC-11 and EC-15, Elk Creek, Nebraska: Molycorp Internal Report.

McDonough, W.F., and Sun, S., 1995, The composition of the Earth: Chemical Geology, v. 120, p. 223-253.

Mitchell, R.H., and Kjarsgaard, B.A., 2004, Solubility of niobium in the system $CaCO_3$–CaF_2–$NaNbO_3$ at 0.1 GPa pressure: implications for the crystallization of pyrochlore from carbonatite magma: Contributions to Mineralogy and Petrology, v. 148, p. 281-287.

Mitchell, R.H., 2014, Primary and secondary niobium mineral deposits associated with carbonatites: Ore Geology Reviews, v. 64, p. 626-641.

Ojakangas, R., Morey, G., and Green, J., 2001, The Mesoproterozoic midcontinent rift system, Lake Superior region, USA: Sedimentary Geology, v. 141, p. 421-442.

P.C.J., compiler, 1985, LnO anomalies, 500 to -300 elevations, Elk Creek: Union76 Molycorp, scale 1":1000', 1 PDF, http://snr.unl.edu/data/geologysoils/mineral/index-mineral.asp.

Powell, R., and Powell, M., 1977, Geothermometry and oxygen barometry using coexisting iron-titanium oxides: a reappraisal: Mineral.Mag, v. 41, p. 257-263.

Seifert, W., Kämpf, H., and Wasternack, J., 2000, Compositional variation in apatite, phlogopite and other accessory minerals of the ultramafic Delitzsch complex, Germany: implication for cooling history of carbonatites: Lithos, v. 53, p. 81-100.

Sherer, R.L., 1984a, Geology of Drill Hole EC-39, Elk Creek, Nebraska: Molycorp Internal Report.

Sherer, R.L., 1984b, Geology of Drill Hole EC-41, Elk Creek, Nebraska: Molycorp Internal Report.

Sherer, R.L., 1984c, Geology of Drill Hole EC-48, Elk Creek, Nebraska: Molycorp Internal Report.

Sherer, R.L., 1983a, Geology of Drill Hole EC-4, Elk Creek, Nebraska: Molycorp Internal Report.

Sherer, R.L., 1983b, Geology of Drill Hole EC-29, Elk Creek, Nebraska: Molycorp Internal Report.

Sherer, R.L., 1981, Petrography of Drill Hole EC-26, Elk Creek, Nebraska: Molycorp Internal Report.

Sillitoe, R.H., 1985, Ore-related breccias in volcanoplutonic arcs: Economic Geology, v. 80, p. 1467-1514.

Sims, P., and Petermar, Z., 1986, Early Proterozoic Central Plains orogen: A major buried structure in the north-central United States: Geology, v. 14, p. 488-491.

Steeples, D.W., DuBois, S.M., and Wilson, F.W., 1979, Seismicity, faulting, and geophysical anomalies in Nemaha County, Kansas: Relationship to regional structures: Geology, v. 7, p. 134-138.

Todd, S., Keith, D., Le Roy, L., Schissel, D., Mann, E., and Irvine, T., 1982, The JM platinum-palladium reef of the Stillwater Complex, Montana; I, Stratigraphy and petrology: Economic Geology, v. 77, p. 1454-1480.

Torró, L., Villanova, C., Castillo, M., Campeny, M., Gonçalves, A., and Melgarejo, J., 2012, Niobium and rare earth minerals from the Virulundo carbonatite, Namibe, Angola: Mineralogical Magazine, v. 76, p. 393-409.

Treiman, A.H., and Schedl, A., 1983, Properties of carbonatite magma and processes in carbonatite magma chambers: The Journal of Geology, p. 437-447.

Williams, C., Wall, F., Woolley, A., and Phillipo, S., 1997, Compositional variation in pyrochlore from the Bingo carbonatite, Zaire: Journal of African Earth Sciences, v. 25, p. 137-145.

Workman, R.K., and Hart, S.R., 2005, Major and trace element composition of the depleted MORB mantle (DMM): Earth and Planetary Science Letters, v. 231, p. 53-72.

Xu, A., 1996, Mineralogy, petrology, geochemistry and origin of the Elk Creek Carbonatite [Ph.D. Thesis]: Lincoln, University of Nebraska, 317 p.

Yegorov, L., 1993, Phoscorites of the Maymecha-Kotuy ijolite-carbonatite association: International Geology Review, v. 35, p. 346-358.

Appendix A

Table A1: Whole-rock major-element and trace-element geochemistry for selected magnetite-dolomite carbonatite and unmineralized carbonatite composite samples.

Field No.			EC-16 1380'	EC-28 1800'	EC-11 2425'	EC-29 1480'	EC-15 1010'	EC-39 2030'	EC-48 2000'	EC-43 810'	EC-4 2400'
Sample Description			Magnetite-Dolomite Carbonatite	Magnetite-Dolomite Carbonatite	Magnetite-Dolomite Carbonatite	Magnetite-Dolomite Carbonatite	Apatite-Dolomite Carbonatite	Apatite-Dolomite Carbonatite	Dolomite Carbonatite	Barite-Dolomite Carbonatite	Syenite
Nb_2O_5	%	ICP-AES	**0.85**	**0.97**	**1.20**	**1.49**	**0.09**	**1.63**	**0.09**	**0**	**0.04**
Ta_2O_5	ppm	ICP-AES	14.65	14.90	7.94	31.99	24.54	279.63	10.99	<0.6	8.06
Major Oxides											
Al_2O_3	%	WDXRF	2.01	2.21	1.96	1.57	0.31	0.59	0.26	0.1	8.65
CaO	%	WDXRF	20.2	18.9	14.7	19.3	29.3	28.9	31.4	22.9	13.4
Cr_2O_3	%	WDXRF	0.03	0.03	0.03	<0.01	<0.01	<0.01	<0.01	<0.01	<0.01
Fe_2O_3	%	WDXRF	12.7	16.7	19.4	21.7	6.79	4.74	6.41	7.62	5.98
K2O	%	WDXRF	1.65	1.73	1.58	1.07	0.2	0.11	0.24	0.04	6.62
MgO	%	WDXRF	10.1	8.6	6.73	11.1	15.3	17	14.9	10.4	5.69
MnO	%	WDXRF	0.66	0.65	0.61	0.64	0.7	0.55	0.81	1.3	0.61
Na_2O	%	WDXRF	0.16	0.29	0.25	0.27	0.08	0.08	0.1	0.08	0.29
P_2O_5	%	WDXRF	0.63	0.31	0.44	0.93	2.13	2.92	4.78	1.36	1.23
SiO_2	%	WDXRF	10.3	9.44	10.9	6.83	1.26	2.13	0.96	11.2	27.9
TiO_2	%	WDXRF	3.07	3.94	5.37	3.91	0.25	0.07	0.14	0.05	0.51
LOI	%	WDXRF	29.3	27.5	20.6	26.7	40.4	0.59	37.5	32.2	8.65
Trace Elements											
Ag	ppm	ICP-AES	<1	<1	<1	<1	<1	<1	<1	<1	<1

As	ppm	ICP-AES	<30	<30	<30	<30	<30	<30	<30	<30	<30
Ba	ppm	ICP-AES	44700	42200	83400	41400	6960	501	441	24800	45600
Be	ppm	ICP-AES	17	17	38	41	<5	19	<5	7	5
Bi	ppm	ICP-AES	1.1	1	0.9	1.3	1.4	<0.1	0.9	0.1	<0.1
Cd	ppm	ICP-AES	0.7	1.5	0.8	0.5	0.7	3.6	<0.2	1.4	0.8
Ce	ppm	ICP-AES	1460	1060	848	790	470	410	1690	25400	4740
Co	ppm	ICP-AES	26.9	27.4	26.9	15.7	17.2	24.2	25	5.3	5.4
Cr	ppm	ICP-AES	210	210	160	120	20	10	<10	<10	<10
Cs	ppm	ICP-AES	0.6	0.2	1.8	<0.1	<0.1	0.2	0.1	<0.1	0.6
Cu	ppm	ICP-AES	79	47	54	48	11	41	37	<5	7
Dy	ppm	ICP-AES	55.2	40.8	24.1	87[1]	14.7	11	42.6	34	18
Er	ppm	ICP-AES	14	10.2	7.68	22.2[1]	4.71	4	14.1	8.53	6.1
Eu	ppm	ICP-AES	46.1	58.1	49.4	71[1]	11.7	8	21.9	69	24
F	ppm	F-ISE	1860	1190	1930	1250	2080	2240	4010	9290	1960
Ga	ppm	ICP-AES	14	20	7	13	3	6	2	<1	14
Gd	ppm	ICP-AES	138	149	94.5	227[1]	29.6	23	60.7	142	52
Ge	ppm	ICP-AES	<1	1	2	3	<1	<1	<1	3	<1
Hf	ppm	ICP-AES	4	4	5	2	<1	3	2	<1	7
Ho	ppm	ICP-AES	6.73	4.84	3.21	11.8[1]	2.12	1.8	6.4	4.36	2.9
In	ppm	ICP-AES	0.5	0.5	1.2	0.8	0.3	<0.2	0.4	0.3	<0.2
La	ppm	ICP-AES	879	588	407	410[1]	187	160	916	19300	3340
Li	ppm	ICP-AES	110	20	20	<10	<10	<10	<10	40	10
Lu	ppm	ICP-AES	1.43	1.08	0.82	1.4[1]	0.4	0.3	0.92	0.63	0.5
Mo	ppm	ICP-AES	20	11	13	8	141	120	53	29	40
Nb	ppm	ICP-AES	5970	6800	8400	10400	620	11400	613	32	258
Nd	ppm	ICP-AES	448	365	300	340[1]	216	180	539	5290	1170
Ni	ppm	ICP-AES	76	77	63	54	12	10	11	<5	6
Pb	ppm	ICP-AES	158	152	42	130	52	426	20	22	16
Pr	ppm	ICP-AES	128	99.4	79.7	90[1]	55.9	50	155	2160	400

Rb	ppm	ICP-AES	25.2	15.2	23.9	11.7	2	4.2	3.1	1.3	88.6
Sb	ppm	ICP-AES	5.4	3.3	4.6	7.8	0.5	1.7	0.3	0.6	0.2
Sc	ppm	ICP-AES	78	72	56	65	17	8	21	18	6
Sm	ppm	ICP-AES	100	118	136	140[1]	40.4	30	76	370	120
Sn	ppm	ICP-AES	15	27	77	25	1	11	4	4	2
Sr	ppm	ICP-AES	2250	3240	2360	1410	3180	3020	1670	3910	2460
Ta	ppm	ICP-AES	12	12.2	6.5	26.2	20.1	229	9	<0.5	6.6
Tb	ppm	ICP-AES	14.9	12.7	6.74	24[1]	3.33	3	8.32	15	5
Th	ppm	ICP-AES	140	430	191	512[1]	72.8	272	109	227	85
Tl	ppm	ICP-AES	<0.5	<0.5	<0.5	<0.5	<0.5	1.9	<0.5	<0.5	<0.5
Tm	ppm	ICP-AES	1.67	1.24	0.96	2.3[1]	0.54	0.5	1.51	0.89	0.7
U	ppm	ICP-AES	46.2	81.1	46.6	88	25.3	208	8.28	13.6	19
V	ppm	ICP-AES	277	265	231	176	54	30	93	58	82
W	ppm	ICP-AES	64	47	72	73	3	1	3	2	2
Y	ppm	ICP-AES	163	125	87.6	273	55.5	41	167	101	60
Yb	ppm	ICP-AES	10.2	7.2	6	12[1]	2.9	2	7.5	4.5	4
Zn	ppm	ICP-AES	696	1200	249	1090	481	723	43	118	51
Zr	ppm	ICP-AES	99.8	67.5	95	48.5	17.9	106	86.4	15.2	486

[1] Analysis by ICP-MS